TAMPEREEN TEKNILLINEN YLIOPISTO
TAMPERE UNIVERSITY OF TECHNOLOGY

TUULIA JOKELA

THERMAL PROPERTIES AND IN VITRO DISSOLUTION OF BIO-ACTIVE BOROSILICATE GLASSES

Bachelor of Science Thesis

Laboratory of Chemistry and Bioengineering
Instructor: Academy Research Fellow Jonathan Massera
Examiner: Docent, University Lecturer Terttu Hukka

ABSTRACT

TAMPERE UNIVERSITY OF TECHNOLOGY
Bachelor of Science in Technology
JOKELA TUULIA: Thermal Properties and In Vitro Dissolution of Bioactive Borosilicate Glasses
Bachelor of Science Thesis, 37 pages, 9 Appendix pages
November 2018
Major: Chemistry
Instructor: Academy Research Fellow Jonathan Massera
Examiner: Docent, University Lecturer Terttu Hukka
Keywords: bioactive glass, borosilicate, thermal properties, dissolution

Tissue engineering and biodegradable implants were developed to avoid problems caused by long-term use of non-metabolizing implants. Tissue engineering aspires to produce new tissues by using the patient's own cells. Commonly, a porous three-dimensional (3D) scaffold is used as a supporting structure until enough new tissue has grown. Typical bioactive silicate glasses have many good qualities, such as their ability to bond to bone by forming a hydroxycarbonate apatite (HCA) layer, but due to their tendency to crystallize during sintering and excessively long dissolution time, more suitable scaffold materials need to be developed.

Borosilicate glasses based on commercial silicate glass S53P4 have emerged as a new and promising scaffold material due to their higher bioactivity and dissolution rate and better resistance to crystallization. In this thesis, three borosilicate glasses based on S53P4 were studied and compared with the S53P4 glass. The glasses' thermal properties, bioactivity and dissolution were studied with differential thermal analysis (DTA), dissolution tests, inductively coupled plasma optical emission spectrometry (ICP-OES) and Fourier transform infrared spectroscopy (FTIR) to evaluate which composition has the most promising properties to be used as a tissue engineering scaffold material. Of these, DTA was used to determine the glasses' ability to be processed at high temperatures by determining their thermal processing window (ΔT). Dissolution tests were conducted by immersing glass particle in simulated body fluid (SBF) and 2-amino-2-(hydroxymethyl)propane-1,3-diol (TRIS) solution for 6–168 h, and then measuring the pH of the solutions after each time point. From the obtained pH curves, dissolution rate and HCA layer formation were observed. Ion release of the glass particles was further studied with ICP-OES and structural changes in the glasses' surface and precipitation of the HCA layer with increasing immersion time were studied with FTIR.

Based on the results, borosilicate glasses dissolve quicker than S53P4 and they form a thicker and more crystallized HCA layer. B50 was the only borosilicate glass to have a wider ΔT than S53P4. Out of the three borosilicate glasses, B50 has the most promising properties concerning its use in tissue engineering as it has the widest ΔT, it dissolves the quickest and it forms the thickest and most crystallized HCA layer on its surface.

TIIVISTELMÄ

TAMPEREEN TEKNILLINEN YLIOPISTO
Tekniikan ja luonnontieteiden kandidaatintutkinto-ohjelma (TkK)
JOKELA TUULIA: Bioaktiivisten borosilikaattilasien termiset ominaisuudet ja liukeneminen
Kandidaatintyö, 37 sivua, 9 liitesivua
Marraskuu 2018
Pääaine: Kemia
Ohjaaja: Akatemiatutkija Jonathan Massera
Tarkastaja: Dosentti, Yliopiston lehtori Terttu Hukka
Avainsanat: bioaktiivinen lasi, borosilikaatti, termiset ominaisuudet, liukeneminen

Kudosteknologia ja biohajoavat implantit kehitettiin, biohajoamattomien implanttien pitkäaikaiskäytöstä aiheutuvien ongelmien välttämiseksi. Kudosteknologia pyrkii luomaan uusia kudoksia potilaan omien solujen avulla. Huokoista 3D-rakennelmaa käytetään usein tukemaan ympäröiviä kudoksia, kunnes uutta kudosta on muodostunut tarpeeksi. Tyypillisillä bioaktiivisilla silikaattilaseilla on monia hyviä ominaisuuksia, kuten kyky sitoutua luuhun muodostamalla hydroksikarbonaattiapatiittikerros (HCA), mutta niillä on kuitenkin taipumus kiteytyä sintrauksen aikana ja niiden hajoaminen on erittäin hidasta, minkä vuoksi soveltuvampien tukirakennemateriaalien kehittäminen on tärkeää.

Kaupalliseen S53P4-silikaattilasiin pohjautuvat borosilikaattilasit ovat nousseet esiin uusina lupaavina materiaaleina, niiden korkeamman bioaktiivisuuden ja liukenemisnopeuden, sekä paremman kiteytymisenvastustuskyvyn vuoksi. Tässä kandidaatintyössä tutkittiin kolmea eri borosilikaattilasia, jotka perustuivat S53P4-lasiin. Lasien termisiä ominaisuuksia, bioaktivisuutta ja liukenemista tutkittiin differentiaalisen termisen analyysin (DTA), liuotuskokeiden, induktiivisesti kytketyn plasma-optisen emissiospektrometrian (ICP-OES) ja Fourier-muunnosinfrapunaspektroskopian (FTIR) avulla, jotta saatiin selville millä lasilla on parhaimmat ominaisuudet käytettäväksi kudosteknologiassa. DTA:ta käytettiin arvioimaan lasien kuumankestävyyttä määrittämällä niiden lämpökäsittelyikkuna (ΔT). Liuotuskokeissa lasipartikkeleita liuotettiin kudosnestettä simuloivassa liuoksessa (SBF) ja 2-amino-2-(hydroksimetyyli)propaani-1,3-dioli (TRIS) liuoksessa 6–168 tuntia, jonka jälkeen liuoksien pH mitattiin. Saatujen pH-kuvaajien avulla tutkittiin lasien liukenemisnopeutta ja HCA-kerroksen muodostumista. Lasipartikkeleista vapautuneiden ionein määrä mitattiin ICP-OES:n avulla. Lasin pintarakenteessa tapahtuvia muutoksia ja HCA-kerroksen muodostumista ajan edetessä tutkittiin FTIR:n avulla.

Tulosten perusteella borosilikaattilasit liukenevat nopeammin kuin S53P4 ja ne muodostavat paksumman ja kiteytyneemmän HCA-kerroksen niiden pinnalle. Lisäksi B50 oli ainoa borosilikaattilasi, jonka ΔT oli suurempi kuin S53P4:n. Tutkituista borosilikaattilaseista B50:llä on lupaavimmat ominaisuudet ajatellen sen käyttöä kudosteknologiassa, koska sillä on suurin ΔT, se liukenee nopeimmin ja sen pinnalle muodostuva HCA-kerros on paksuin ja kiteytynein.

TABLE OF CONTENTS

LIST OF SYMBOLS AND ABBREVIATIONS

ATR	Attenuated total reflectance
B	Boron
B_2O_3	Boron trioxide
Ca	Calsium
CaO	Calsium oxide
DTA	Differential thermal analysis
FTIR	Fourier transform infrared spectroscopy
HA	Hydroxyapatite
HCA	Hydroxycarbonate apatite
ICP-OES	Inductively coupled plasma optical emission spectrometry
MgO	Magnesium oxide
Na	Sodium
Na_2O	Sodium oxide
P	Phosphorus
pp	Percentage point
P_2O_5	Phosporus pentoxide
SBF	Simulated body fluid
Si	Silicon
SiO_2	Silica
TRIS	2-Amino-2-(hydroxymethyl)propane-1,3-diol
T_g	Glass transition temperature
T_p	Peak of crystallization temperature
T_x	Onset of crystallization temperature
3D	Three-dimensional
ΔT	Thermal processing window
ΔT_{DTA}	Temperature difference between a sample and a reference

1. INTRODUCTION

A biomaterial is defined as a "material intended to interface with biological systems to evaluate, treat, augment or replace any tissue, organ or function of the body" by the European Society for Biomaterials [1]. Biomaterials include e.g. ceramics, metals, plastics and materials from biological sources [2]. In the beginning of the development of biomaterials the most important criterion of an implant was that it would be biologically inert. Biologically inert implants are passive constructions that support and replace tissues. In long-term use (10–20 years), non-metabolizing implants can cause problems, because metals can corrode, and plastics expire and become brittle. Both phenomena can cause chronic infections, pain, swelling and loosening or removal of an implant from body. To avoid these problems biodegradable implants were developed, and the research to improve existing implants and develop new ones is ongoing. The advantages of biodegradable implants are that they support or replace tissues until the tissues are healed, and then metabolize away before causing any long-term complications. Most biodegradable implant materials act passively but some materials, like certain glasses, are bioactive which accelerates the healing of damaged tissue. [3]

A material is bioactive when it evokes a positive reaction at the tissue-material interface, which leads to the formation of a bond between the material and the surrounding tissues. A bioactive glass is a ceramic made, most commonly, from silica (SiO_2), sodium oxide (Na_2O), calcium oxide (CaO) and phosphorus pentoxide (P_2O_5). [4] The first bioactive glass was developed by Larry Hench in 1969. Before participating in a research project funded by the US Army, Hench was researching semiconductors at the University of Florida. Hench and his team's discovery of radiation resistant electronic materials led him to an US Army conference in 1967. On his way to the conference Hench met an Army colonel who, after listening to Hench's discoveries about materials that can withstand exposure to high-energy radiation, asked Hench would it be possible to make a material that would tolerate the conditions inside a human body. The colonel further explained that current materials e.g. metals and polymers caused scar tissue to form around an implant, which increased the likelihood of the implant to be rejected by the body. Intrigued by the colonel's sayings Hench wanted to start developing materials that, instead of eliciting scar tissue growth, would form a bond with the surrounding tissues (osseointegrate). [5, 6] After the conference Hench pitched the idea to his friend and together they submitted the research project idea to the US Army, which later resulted in the discovery of the first bioactive glass, 45S5 (Bioglass®). Bioglass® is composed out of SiO_2 (46.1 mol-%), CaO (26.9 mol-%), Na_2O (24.4 mol-%) and P_2O_5 (2.6 mol-%). This specific composition was chosen because it is close to the ternary eutectic in a Na_2O-CaO-SiO_2 diagram. [5]

Bioactive glasses can bond with bone tissue by forming a hydroxycarbonate apatite (HCA) layer which then interacts with the surrounding tissues and molecules. Due to their bone bonding ability, bioactive glasses are most commonly used in bone applications. [7]

Tissue engineering is a multidisciplinary field which started in the US in the late 1980's and has since been growing. Tissue engineering combines porous three-dimensional scaffolds that can be made, for example, from bioactive glass, with cells and growth factors to create structures that support and

replace tissues and stimulate new tissue growth until the tissue is healed. As new tissue grows, the scaffold degrades and finally, when the tissue is fully healed, the scaffold has completely degraded away. [3, 8] Bioactive glasses are often sintered into 3D-scaffolds, but the problem with silica glasses is that they start to crystallize in the temperatures used in sintering, which then decreases their bioactivity [9, 10]. To decrease crystallization tendency and to improve bioactivity, many compounds, such as boron trioxide (B_2O_3) and magnesium oxide (MgO) have been added to the already existing silicate glass compositions, such as S53P4 (BonAlive®) [11, 12].

The aim of this Bachelor of Science thesis is to study three different borosilicate glasses: B12.5, B25 and B50 that are based on a silicate glass, S53P4. The studied properties were the glasses' in vitro dissolution and thermal properties, and the aim was to determine which borosilicate glass composition has the best properties concerning its use as a tissue engineering scaffold material. The best properties are defined as the glass having a wider thermal processing window and a higher dissolution rate than S53P4 and the glass forms the thickest and most crystallized HCA layer. To determine which borosilicate glass composition seems most promising, the glasses' thermal properties were studied to determine their thermal processing window. Dissolution rate and HCA layer formation were studied with dissolution tests, by measuring the ionic concentration of the immersion solutions after certain time points and by studying the structural changes in the glasses' surface layer.

In the second chapter of this thesis, the theorical background of bioactive glasses is described. First the properties of silicate glasses are addressed and then how adding boron affects the glass properties. The third chapter describes the sample preparation and methods used to study in vitro and thermal properties of the selected glasses. In the fourth chapter, the results are presented, analyzed and discussed. The fifth and final chapter has the conclusions of this study.

2. THEORETICAL BACKGROUND

This chapter first describes the basics of glass structure and its properties. Then the dissolution process, thermal properties and applications of bioactive glasses are explained. Last the effects of boron addition in bioactive glass properties are addressed.

2.1 Glass Properties and Structure

Glasses are amorphous materials, which means that the atoms in the lattice have no long-range order unlike in crystalline materials [11, 13]. Due to their amorphous structure glasses do not have a precise melting point, but they soften over a temperature range [14]. Another characteristic of amorphous materials is glass transition which will be explained in detail in Section 2.5. Below glass transition glasses are hard materials, so they have good abrasion resistance but, on the other hand, glasses are also brittle and vulnerable to stress concentrations which complicates their use in load-bearing applications [11, 15].

The basic components of a glass structure are network formers, network modifiers and intermediate oxygens. Network formers like SiO_2, P_2O_5 and B_2O_3 form the basis of a glass by connecting to each other via oxygen atoms called bridging oxygen atoms. In silica glasses the silica atoms are connect to four oxygen atoms creating a 3D-structure. Network formers can be the only components in a glass network, but usually there are also network modifiers and intermediate oxides in the structure. Network modifiers are e.g. alkali and alkaline earth metal cations (Na^+, K^+, Ca^{2+}) that disrupt the glass structure by turning the bridging oxygen atoms into non-bridging oxygen atoms. Covalent bonds connecting the oxygen atoms to other atoms turn predominantly into ionic linkages (Si-O-Si → Si-O^- M^+, where M^+ is a network modifier cation). [11] With silicate-based glasses, when the covalent cross-linking deceases due to the increase of network modifiers, the glass's softening temperature decreases. The glass also become chemically more unstable, which enables atoms to move around more at elevated temperatures, increasing the glasses' tendency to crystallize. [16] Intermediate oxides, on the other hand, can behave like typical network modifiers or can potentially enter the backbone of the glass structure and behave almost like network formers. Although, intermediate oxides complicate the glass structure because they can switch their role in the glass, they can, for example, decrease the tendency of a bioactive glass to crystallize. [11]

Network connectivity tells how many bridging oxygen atoms there are per network-forming component in the glass structure, i.e. how cross-linked the glass network is. Glasses with low network connectivity have a lower glass transition temperature (T_g), higher solubility and higher reactivity than glasses with higher network connectivity. Network connectivity of bioactive glasses is usually 2–3. [11, 17]

2.2 Bioactivity and Dissolution of Bioactive Glasses

Bioactivity of a material is defined as the ability of bioactive materials to evoke a positive reaction at the tissue-material interface, which leads to the formation of a bond between the material and the

surrounding tissue [4, 8]. There are three features, which separate bioactive glasses from conventional ones. Bioactive glasses contain less than 60 mol-% of SiO_2, they have high Na_2O and CaO content, and a high CaO/P_2O_5 ratio, which leads them to have a highly reactive surface when exposed to an aqueous medium [18]. Bioactive glasses form a bond with the surrounding tissue by forming an HCA layer. There are five stages in the HCA layer formation, in body fluid in vivo (inside of body) or in simulated body fluid (SBF) in vitro (outside of body), for silicate-based glasses. Glasses that contain less silica have a lower network connectivity and therefore dissolve more rapidly meaning that the following stages happen more quickly. [7] In stage 1, network modifiers exchange ions (Na^+, K^+, Ca^{2+} with H^+ or H_3O^+) with the surrounding body fluids or SBF. Silica groups in the glass network hydrolyze because of the rapid ion exchange. [4, 8]

$$\mathrm{Si{-}O{-}Na^+ + H^+ \rightarrow Si{-}O - H^+ + \ Na^+\ (aq)} \qquad (1)$$

In stage 2, because of the hydrolysis pH of the surroundings increases it leads to the dissolution of SiO_2, formation of silicic acid ($Si(OH)_4$) into the solution and the formation of Si-OH (silanols) on the glass surface. [4, 8]

$$\mathrm{Si{-}O{-}Si + H_2O \ \rightarrow Si{-}OH + Si{-}OH} \qquad (2)$$

In stage 3, the amorphous SiO_2-rich layer condensates and polymerizes on the surface of the glass, which is depleted in alkalis and alkaline earth cations. [4, 8]

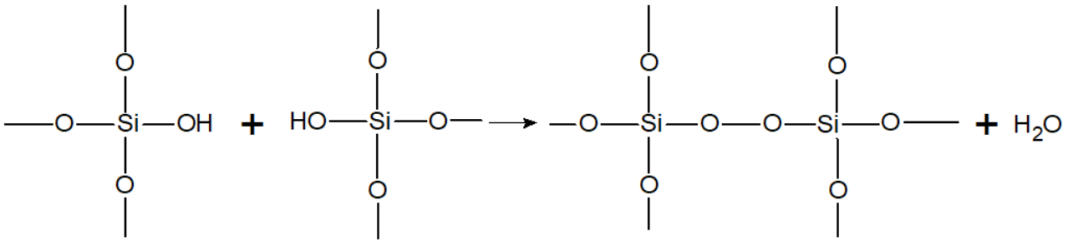

(3)

In stage 4, the dissolution process of the glass network continues, and Ca^{2+} and PO_4^{3-} ions from the glass network migrate through the SiO_2-rich layer and form a $CaO\text{-}P_2O_5$-rich layer on top of it. After the $CaO\text{-}P_2O_5$-rich layer has formed, it grows by obtaining the soluble Ca^{2+} and PO_4^{3-} ions from the surrounding solution and connects them into the existing structure. [4, 8]

In stage 5, the glass network dissolves further and the $CaO\text{-}P_2O_5$-rich layer crystalizes. The $CaO\text{-}P_2O_5$-rich layer crystalizes to an HCA layer by intaking OH^-, CO_3^{2-} ions from the solution. [4, 8] Bioactive glasses precipitate primarily into HCA instead of hydroxyapatite (HA) in SBF because SBF is supersaturated towards HCA precipitation [19, 20].

The increase of pH due to the ion exchange in stage 2 causes bioactive glasses to have antibacterial properties. It has been shown that S53P4 has growth-inhibiting properties towards 17 anaerobic bacteria and 29 clinically important aerobic bacteria in vitro. In addition, S53P4 exhibits antibacterial properties in lower concentrations and it has the fastest killing or growth-inhibiting effect towards anaerobic bacteria compared to 13-93 and CaPSiO II bioactive glasses. [11, 21, 22] Products that come from the degradation and dissolution of bioactive glasses induce osteoinduction [7]. In osteoinduction, dissolution products stimulate genes that in turn stimulate progenitor cells to differentiate into osteoblasts (cells that produce bone), and, as a result, new bone is formed (osteogenesis) [6, 23].

Other terms related to the bioactivity and bone formation are osteoconductivity and osteostimulation. Osteoconductive glasses provide a surface along which or into the bone tissue, blood capillaries and perivascular tissue can grow, whereas glasses that are osteostimulation can improve and actively stimulate proliferation and differentiation of progenitor cells. [6, 24, 25]

2.3 Applications of Bioactive Glasses

Bioactive glasses are commonly used in tissue engineering. Tissue engineering is a multidisciplinary field that combines e.g. cellular biology, material sciences and biochemistry in creating new tissues and organs from patient's own cells [3]. Most commonly, a porous 3D-scaffold is produced from a biodegradable material in which cells and/or growth factors can be incorporated either outside the body (in vitro) or inside the body (in vivo or in situ) [3, 8]. Other scaffold materials besides ceramics are synthetic and natural polymers [1].

Bioactive glasses are most commonly used in bone repair applications because of their ability to form HCA, which closely resembles crystalline HA found in bones [17, 26]. Bone is the second most transplanted tissue after blood, and usually autografts are used. Autografts are grafts that are taken from another part of the patient, which means that there is no risk of foreign body reaction. [7, 27] Allografts, in turn, are taken from a different individual of the same species, while xenografts are taken from a different species. Both allografts and xenografts can cause a foreign body reaction. [28–30]

Foreign body reaction occurs at the end-stage of an inflammatory and wound healing process in which a fibrous capsule is formed around a foreign object e.g. biomaterial or an implant [30]. The fibrous capsule that isolates the object from the surrounding tissues, and prevents it from spreading, forms because the body's immune system cannot eliminate the intruder by phagocytosis or phagolysosomal digestion [31]. It is critical to understand the mechanism of foreign body reaction because it can affect the biocompatibility, safety and function of a device, implant or a tissue-engineering structure [30]. While there are many advantages in using allografts, such as having no risk of foreign body reaction as mentioned previously, the downside of using allografts is their limited supply and pain caused to the donor site due to extraction operation [7, 27].

There are many criteria for a bioactive glass scaffold. The scaffold must be biocompatible, which is defined as the scaffold fulfilling its intended purpose of supporting cellular activity, to maximize tissue regeneration without eliciting adverse effects at a local or systemic scale [32]. The scaffold needs to degrade into non-toxic products that can be metabolized away at the same rate as the new tissue is formed [8]. The mechanical properties need to match the tissue that the scaffold is going to replace, and the scaffold should maintain its mechanical strength until enough new tissue is formed. To allow cell penetration and diffusion of nutrients and waste to and away from the cells, the porosity of the scaffold needs to be at least 50 %, preferably over 90 % and the pore size at least 100 μm, preferably 100–500 μm. In addition, the pores need to be interconnected. [8, 10] The scaffold material must allow processing into relevant shapes, manufacturing of the scaffold should be cost-effective, and the manufacturing process must be suitable for small- and large-scale production. Finally, the finished scaffold must be capable of being sterilized. [1, 8]

2.4 Sintering and Thermal Properties of Glasses

One method of producing bioactive glass scaffolds is sintering. Sintering is needed when scaffolds are made from glass particles in order to fuse the particles together to form a solid structure [7]. In viscous sintering, a powdered glass is heated close to, or above its softening temperature, and then compressed to form a solid structure [33]. The densification is caused by viscous flow. Surface tension gradients drive the material flow towards the particle necks, and eventually the particles combine decreasing the porosity and shrinking the powder compact. [34] Parameters that affect the sintering process and the characteristics of the final product are, for example, processing temperature, material composition, and particle size and packing [33].

Thermal analysis is an analysis method intended for measuring the change of a physical property as a function of temperature in a temperature-controlled environment [35]. One method of analysis is differential thermal analysis (DTA, also called heat flux DSC). Properties that can be measured with DTA are, for example, glass transition temperature, onset temperature of crystallization and melting point. [36]

In glass transition, liquid transforms to a glass, over a temperature range, when cooled rapidly [37]. The cooling rate needs to be fast enough to prevent the material from reaching an equilibrium at any temperature, which would lead to the formation of crystals [38]. When cooled down enough the long-range motion of molecule chains becomes prevented [39]. Glass transition temperature (T_g) is a temperature where the viscosity of the material is 100 TPa [40]. Glassy state is a metastable state, meaning that the system is not in an equilibrium and its lifetime is exceptionally long compared to excited states of atoms [41]. The thermodynamically stable state for a glassy material at low temperatures is crystalline solid. Glass transition changes the properties of glass, such as the heat capacity and thermal expansion coefficient. [38]

Crystallization begins with nucleation, which then leads to the formation of crystals [42]. Nucleation starts at a temperature where the viscosity of the glass melt is low enough to allow atomic rearrangement and diffusion. Before crystals can form, the nuclei need to reach a critical radius to become stable. Nuclei with a radius smaller than the critical value dissolve due to their unstable nature. The critical radius increases as the temperature increases, leading it to be infinite at melting point. Crystallization starts when nuclei have reached the critical size and the temperature is high enough for the atoms to rearrange into an ordered structure i.e. crystals. [43]

2.5 Thermal Properties of Silicate-based Bioactive Glasses

Typical silicate bioactive glasses crystallize easily during hot processing [9, 10]. Temperatures used to hot process the glasses causes them to crystallize which means that it is not possible to fully sinter them before crystals start to form [10]. One of the reasons why bioactive glasses tend to crystallize relatively easy is because of the glass network's low network connectivity due to a large concentration of non-bridging oxygen atoms. The large amount of oxygen atoms reduces the covalent cross-linking between the silicate chains, which enables the structural units to move around more, which further advances the formation of critical size nuclei. [11]

Silicate glasses crystallize into silica phases, and it has been found that S53P4 crystallizes into two different crystalline phases because of their low phosphate content, which, in turn, decreases their bioactivity and solubility [9-11, 44]. Bioactivity and solubility decrease when the degree of crystallinity increases, because the molecules in the crystals are organized into an ordered structure which restricts the movement of the amorphous regions, thereby preventing molecules to pass through the material surface which delays the HCA layer formation (in SBF) [45, 46]. In addition, the crystallized areas in a glass increase the network connectivity of the remaining glass phase. Some secondary crystalline phases have even been found to be insoluble in SBF and 2-amino-2-(hydroxymethyl)propane-1,3-diol (TRIS) solution. Crystallization also decreases the reaction rate and causes an uncontrollable release of ions. [10]

The ability of a bioactive glass to be processed at high temperatures can be roughly approximated by calculating the temperature difference between the onset of crystallization (T_x) and the glass transition temperature (T_g). This temperature range in which viscosity allows sintering and other processing methods is called the thermal processing window (ΔT). [11] A large ΔT predicts that viscous flow happens before crystallization, and if a bioactive glass has a small ΔT, then the nucleation and crystallization are more likely to happen prior, during or after sintering because they are so close to the T_g [45].

The tendency of a bioactive glass to crystallize can be reduced in many ways. One way is by increasing their network connectivity, but if the network connectivity is too high, then the bioactivity and solubility of the glass start to decrease. Another way is to reduce the amount of alkaline and alkaline earth metal cations in the structure. The reduction of these network modifiers lowers the T_g and increases the T_x which leads to a larger ΔT. With a higher number of components in the glass, it is possible to increase entropy of mixing which raises activation energy of critical size nuclei formation, and thereby hinders the crystallization. Adding intermediate ions, such as magnesium, strengthens the bonds in the glass structure which widens the ΔT but it also increases the network connectivity which, after a certain point, starts to decrease the glass's solubility and degradation, as mentioned before. [11] A more recent method is to add B_2O_3, another network former, into the composition. Borosilicate glasses have a lower crystallization rate than silicate (and boron) glasses, which increases their possibility to be sintered without crystallizing [10]. Section 2.6 explains more in detail how the addition of boron affects the crystallization of glass.

2.6 Borosilicate Glasses

Bioactive borosilicate glasses are silica-based and they contain boron trioxide (B_2O_3) [47-51]. Because of boron (B), borosilicate glasses have lower chemical durability than silicate glasses, which is caused by the replacement of SiO_2 with B_2O_3. Boron has a coordination number of 3 which means that it cannot fully form a three-dimensional network like silicon (Si) [47, 49, 52]. Lower chemical durability speeds up the dissolution process, which leads to a more complete conversion to HCA compared to other silicate-based bioactive glasses [47-49]. Although borosilicate glasses do not fully convert to HCA, the sodium (Na) and boron ions in the unconverted glass dissolve entirely into the surrounding solution, so that in the end there is a sodium and boron ion depleted SiO_2-rich core which is surrounded by an HCA layer [47, 48]. The conversion of borosilicate glasses is initially controlled by dissolution of the glass and later by diffusion. As borosilicate glasses dissolve in SBF, basic alkalis

and alkaline earth cations (Na^+ and Ca^{2+}) and hydroxide from the hydrolysis of silica are released. In addition, BO_3^{3-} ions are released into the surrounding solution from the hydrolysis of borate sites in the glass structure, and PO_4^{3-} ions are taken in from the solution to form a $CaO\text{-}P_2O_5$-rich layer. As boric acid is a weaker acid than phosphoric acid pH of the surrounding solution increases. [49] In solutions that do not contain PO_4^{3-}, the increase in pH is due to the hydrolysis of borate and silica in the glass network and the release of basic alkalis and alkaline earth cations [53].

It has been found that while the conversion rate to HCA is greater for borosilicate glasses than silicate-based glasses, the boron ion concentrations higher than 0.65 mmol (in solution) mmol decrease the proliferation of osteoblast-like cells and the growth and proliferation of bone marrow cells. The decrease is due to the toxic nature of the boron leached from the glass. [54] However, the boron released from bioactive glasses has shown no toxic effects in vivo [8, 55]. The ability to support cell differentiation and proliferation in vitro can be increased by mixing the cell culture by shaking it to make the system more dynamic. Another way is to convert the surface layer of the borosilicate glass to HCA by pre-reacting it in an aqueous phosphate solution before adding it to the culture medium. [8] Boron concentrations under 0.65 mmol support the proliferation of bone marrow stromal cells and the proliferation and function of osteogenic MLO-A5 cells in vitro [50, 51]. In addition to stimulating angiogenesis (formation of new blood vessels) in vivo and in vitro, boron released from the dissolution of borosilicate glasses also increases the proliferative and migratory response, tubule formation capacity and secretion of pro-angiogenic cytokines of human umbilical vein endothelial cells in vitro [11, 55]. Boron released from the dissolution of borosilicate glasses supports soft tissue infiltration and extra cellular matrix formation in vivo and enhances bone formation more than silicate glasses [50, 51]. In addition, it has been found that at least borosilicate glass 13-93B1 can fully convert to HCA in vivo [51].

Borosilicate glasses crystallize into silicate phases, and it has been found that probably all borosilicate glasses form at least two different crystal phases when crystallizing [10]. Borosilicate glasses crystallize primarily from the surface and crystallization is most likely surface-controlled rather than diffusion-controlled [10, 11, 45]. Surface crystallization has two main downsides. The first one is that the crystals at the surface will be in contact with the solution. If the crystals are too stable, the solution will not be able to hydrolyze the amorphous phase. [56, 57] The second downside is that surface crystallization can inhibit viscous flow, thereby making sintering more difficult [11]. Borosilicate glasses based on S53P4 generally have a wide thermal processing window and a low activation energy for viscous flow, which makes them suitable for processing via sintering [10]. In a study [45], it was found that at least S53B50 can be sintered without it crystallizing. When compared to silicate glasses, borosilicate glasses have lower T_g, T_x, T_p and forming temperature due to the addition of B_2O_3. B_2O_3 is unable to form a fully 3D-glass network causing the network to be more loosely packed. [10, 47]

The tendency of a borosilicate glass to crystallize can be decreased by using a large particle size because small particle size increases crystallization by increasing the surface nucleation sites [45]. The amount of added alkali oxides, alkaline earth oxides and boron can also influence glass properties. B_2O_3 can appear in two forms trigonal planar [BO_3] and tetrahedral [BO_4] depending on the glass composition. When alkali oxides, such as Na_2O or K_2O, are incorporated into the glass network, the trigonal [BO_3] units convert to tetrahedral [BO_4]. The conversion from [BO_3] to [BO_4] happens only up to a certain alkali oxide concentration after which the number of non-bridging oxygens increases

reversing the changes in properties caused by the [BO_4] units. [BO_4] units increase the network connectivity of the glass structure, which decreases the glasses solubility and bioactivity. This behavior of borate containing glasses is called boron anomaly. The conversion of [BO_3] to [BO_4] and increase of non-bridging oxygens can also happen when alkaline earth oxides are incorporated into the glass network. [58–60] In addition, glasses with only [BO_3] units have shown to have better resistance to crystallization. The amount of B_2O_3 effects the conversion of [BO_3] to [BO_4] in a way that in smaller quantities, B_2O_3 appears in [BO_3] form in the glass but when the B_2O_3 quantity is increased the [BO_3] units transform into [BO_4]. [59] It has also been found that only a small number of the [BO_3] and [BO_4] units are incorporated into the silica network. Due to the phase separation, it can be said that the glass network contains silicate and borate sub-networks. [58]

3. EXPERIMENTAL PART

In this chapter, the methods and procedures used to conduct the experiment are presented. First, the manufacturing of the glass samples is explained, and after that, the different methods used to study the in vitro dissolution and thermal properties. The goal of this experimental part was to determine how the addition of B_2O_3 to S53P4 glass affects the properties of glass and which composition: B12.5, B25 or B50 has the best properties when considering their potential use as tissue engineering scaffold.

3.1 Preparing the Glass Samples

The glass samples were prepared by mixing 99.4 % pure SiO_2 in the form of Belgian quartz sand and analytical grades of H_3BO_3, Na_2CO_3 and $NH_4H_2PO_4$ or $CaHPO_4 \cdot 2H_2O$ from Sigma-Aldrich and $CaCO_3$ from ThermoFisher GmbH. The borosilicate glass samples were made by substituting 12.5, 25 or 50 % of the SiO_2 with H_3BO_3 in the S53P4 glass. The S53P4 glass was used a reference material and prepared along with the other samples.

Before the melting process all the components were mixed and grinded further in mortar. The glasses were melted in a platinum crucible in an LHT 02/07 LB furnace (Nabertherm GhmB, Lilienthal, Germany) by heating them up to 1250 – 1400 °C depending on the glass composition. After that the melted glass was cast onto a graphite mold and put into a pre-heated electrical oven (L 5/11 or L 3/12, Nabertherm) for 5 h at 500 °C for annealing. Annealing is done to release internal stresses and instabilities that form inside the glass due to rapid cooling and would then complicate further processing [61, 62]. After the annealing was done, the glass samples were left to cool down to room temperature inside the oven. Compositions of the glass samples in mol-% are presented in Table 1 and the complete thermal processing cycle is presented in Table 2.

Table 1. *Compositions of the glass samples in mol-%.*

Oxide type	S53P4	B12.5	B25	B50
SiO_2	55.76	47.12	41.84	27.90
B_2O_3	-	6.73	13.95	27.88
CaO	18.99	21.77	18.99	18.99
Na_2O	23.47	22.66	23.46	23.46
P_2O_5	1.78	1.72	1.76	1.78

Table 2. *Thermal processing cycle of the glass samples.*

Step	Time (min)		Final temperature (°C)
Heating (10 °C/min)	60		650
Holding	30		650
Heating (10 °C/min)	20		850
Holding	30		850
		Glass	
Heating to melting temperature (10 °C/min)	55	S53P4	1400
	50	B12.5	1350
	45	B25	1300
	40	B50	1250
Holding	45		At melting temperature
Casting into a graphite mold and transferring into a pre-heated electrical oven.			
Annealing	300		500
Cooling	Over night		Room temperature

In the last sample preparation step, the glasses were crushed in a metal mortar and then sieved with test sieves (Fritsch GmbH, Idar-Oberstein, Germany) to 125–250 µm particles. A Retsch AS 200 sieve shaker (Retsch GmbH, Haan, Germany) was used to separate the glass particles

3.2 Differential Thermal Analysis

Thermal properties of the glass samples were studied with differential thermal analysis (DTA). DTA measures the temperature difference between a sample and a reference (ΔT_{DTA}) which are placed symmetrically in a furnace, which is then heated at a constant rate. The temperature difference is measured by two thermocouples, one in contact with the sample crucible and the other with the reference crucible. ΔT_{DTA} changes from zero to either positive or negative when thermal events, such as crystallization or melting, occur in the sample. If the thermal event is endothermic (absorbing heat), then the ΔT_{DTA} is negative and if the event is exothermic (releases heat), the ΔT_{DTA} is positive. [63] The direction of endothermic or exothermic events depends on the machine and in graphs it is marked with an arrow. Then the obtained ΔT_{DTA} is converted to heat flow rate (dq/dt) with calorimetric calibration and it can be presented as a function of time or temperature [64]. The DTA curves of the samples were measured using a STA 449 F1 Jupiter® (Netzsch-Gerätebau GmbH, Selb, Germany) by placing 30 mg of sample inside a platinum-rhodium crucible with a lid placed on top of it and heating it up to 1250 °C at a 10 °C/min heating rate in a nitrogen atmosphere. The purity of the nitrogen gas was 99.95 % and the flow rate inside the DTA chamber was 20 ml/min. In addition, a 20 ml/min protective nitrogen gas flow was used to protect the balance from any corrosive fumes. An empty crucible was used as a reference.

T_g, T_x and T_p were determined from the DTA curves and then ΔT ($\Delta T = T_x - T_g$) was calculated using the obtained data. An example of a DTA curve and methods used to determine the temperatures in

question are presented in Figure 2. In all the DTA figures obtained from the measuremts the exothermic events are upwards and the endothermic events are downwards.

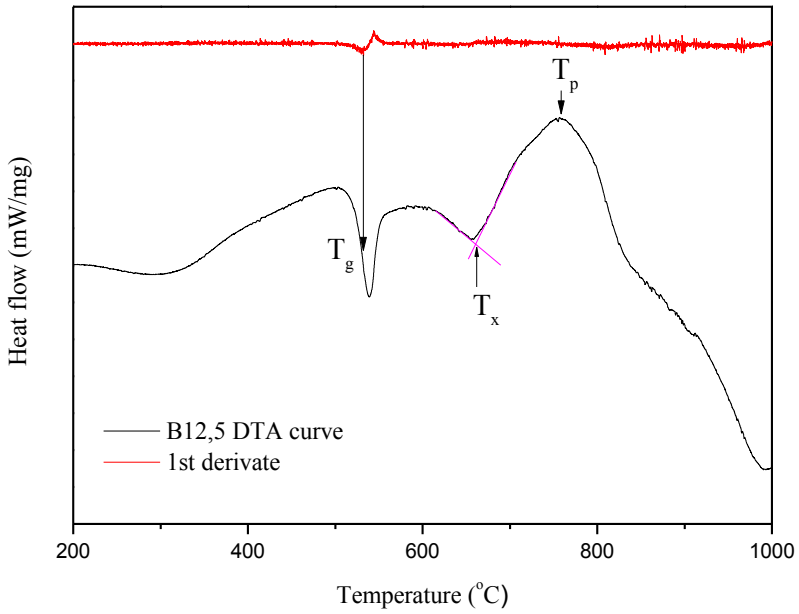

Figure 2. *DTA curve of B12.5 glass showing the determination methods of T_g, T_x and T_p.*

T_g was defined as the inflection point of the first order deviation in the thermogram. The inflection point is measured at the minimum of the DTA curve's first derivate. T_x was determined from the intersection of tangents of the plateau and the crystallization peak following it. T_p was obtained as the maximum of the crystallization peak.

3.3 In Vitro Dissolution

In vitro bioactivity and dissolution behavior of the glass samples were studied by means of dissolution tests conducted in SBF and in TRIS buffer solution. The SBF solution was prepared by following the protocol presented by Kokubo et. al (Shown in appendix A) [65]. One liter of TRIS (pH ~7.4/37 °C) was prepared by dissolving 1.66 g of 2-amino-2-(hydroxymethyl)-1,3-propanediol and 5.72 g of tris(hydroxymethyl)aminomethane hydrochloride into distilled water. Dissolution tests were carried out by immersing 75 mg of each glass in 50 ml of SBF or TRIS for 6, 24, 48, 72 or 168 hours in a 37 °C incubator (Termaks B 8133, Bergen, Norway). Each glass composition had three parallel samples and the pH of the SBF and TRIS solutions without any glass particles was monitored with two control samples at each time point. After each time point, the pH of the sample solutions was measured at 37 ± 0.2 °C with S47-K SevenMulti™ pH-meter (Mettler-Toledo LLC, Ohio, USA). One milliliter of each sample solution was pipetted into a centrifuge tube for inductively coupled plasma optical emission spectrometry (ICP-OES) and the remaining glass particles were filtered with suction filtration and dried for the Fourier transform infrared spectroscopy (FTIR).

3.4 Inductively Coupled Plasma Optical Emission Spectrometry

The concentration of released ions in the SBF or TRIS solution after each time point was measured with ICP-OES 5110 (Agilent Technologies, California, USA). ICP-OES measures the intensity of light emitted by excited ions in the sample solution, which depends on the concentration of the ion. The wavelength of the emitted light is characteristic to each element. Radio frequency current created by a generator causes an oscillating magnetic field. This created electromagnetic field ionizes argon gas and accelerates the released electrons flowing inside the plasma torch. When using liquid samples, the sample solution is transformed into a liquid aerosol by pumping it through a nebulizer into the high-speed argon gas flow. Collisions between the sample ions and electrons causes the ions to become excited. When the ions go back to the ground state, they emit light, of which intensity is related to the concentration of the ion. [66, 67]

For the ICP-OES a specific wavelength was chosen for each element, which are presented in Table 3.

Table 3. *Measured wavelength for each element.*

Element	B	Ca	Na	P	Si
Wavelength (nm)	249.678	422.673	589.592	253.561	250.690

Samples for the ICP-OES were prepared by pipetting 1 ml of each sample solution from the dissolution tests at each time point into a 15 ml centrifuge tube and diluted with 9 ml of 1 M nitric acid to ensure that all the components stay dissolved and do not precipitate [68]. Nitric acid is used because it does not cause chemical or spectral interferences and most elements used in bioactive glasses are soluble in it [69].

3.5 Fourier Transform Infrared Spectroscopy

Structural changes in the glass particles during the dissolution process were monitored by measuring the spectrum with FTIR. In FTIR the infrared radiation is guided through an interferometer (usually a Michelson interferometer). Michelson interferometer consists of three components: a source of IR radiation, a stationary mirror, and a moving mirror. The two mirrors are perpendicular to each other and in the middle of the three components there is a beam splitter. The beam splitter transmits half of the coming radiation to the stationary mirror and reflects the other half to the moving mirror. After the two radiation beams reflect off their respective mirrors they recombine at the beam splitter, as presented in Figure 3. [70, 71]

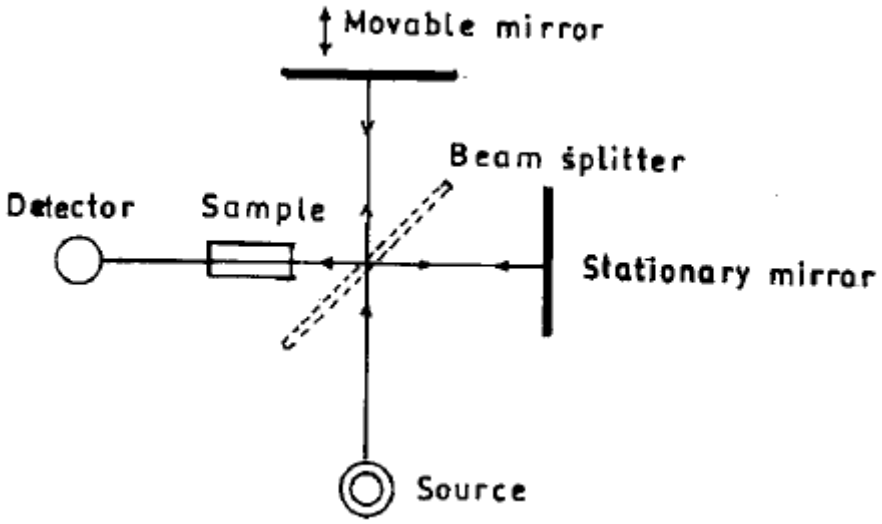

Figure 3. *Diagram of a Michelson interferometer [72].*

The path length of the radiation varies depending on the position of the moving mirror. When the two beams recombine at the beam splitter they interfere with each other either constructively or destructively depending on the path length differences. Next, the recombined beam leaves the interferometer and interacts with the sample before striking a detector. The frequency of the infrared radiation changes at a specific rate and if the dipole moment of a molecule changes at the same rate as the frequency, the infrared radiation is absorbed by a bond in the molecule. The intensity of an absorbance peak must exceed a certain threshold value before it can be detected. Radiation frequencies not absorbed by the sample reach the detector producing an interferogram. In the interferogram the intensity of the absorbance (or transmittance) is plotted as the function of the path length difference, also known as retardation. To get the data into an interpretable form, Fourier transformation is used to convert the signal from time domain into frequency domain. When the signal is in frequency domain, a plot of intensity as a function of frequency, or more commonly wavenumber, known as spectrum, can be produced. [70, 71]

The FTIR spectra of the glass samples were measured before and at each immersion time point of the dissolution tests with a Spectrum One FT-IR Spectrophotometer (PerkinElmer Inc., Massachusetts, USA) using an attenuated total reflectance (ATR) accessory. The spectra were measured between 650–4000 cm^{-1} and 8 accumulations scan were conducted with a 4 cm^{-1} resolution. The obtained spectra were background corrected and normalized to the peak with the highest intensity.

4. RESULTS AND DISCUSSION

In this chapter, results from the experimental part are presented and analyzed. Results from different glass compositions are compared to one another in order to find out which composition has the most promising results to be used as a tissue engineering scaffold.

4.1 Thermal Properties

DTA measurements were conducted to see how B_2O_3 addition affects the glasses' ΔT. The DTA curve for each glass composition is presented in Figure 4. Thermal parameters T_g, T_x, and T_p as well as the thermal processing window determined from the DTA curves are presented in Table 4.

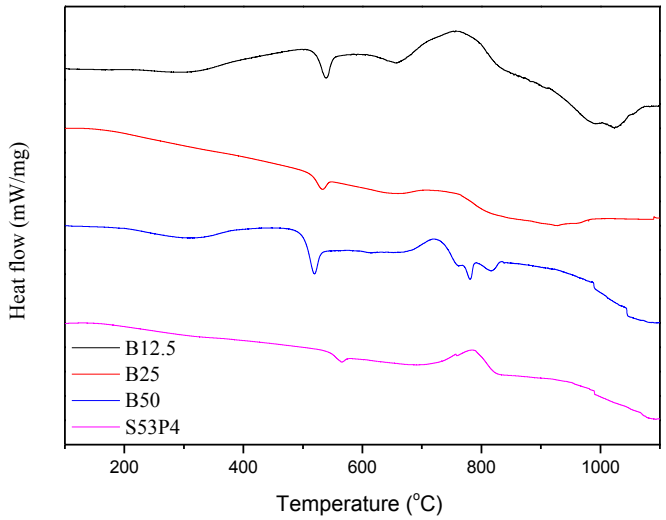

Figure 4. *DTA curves of the glass samples.*

Table 4. *Thermal parameters (T_g, T_x and T_p) and thermal processing window (ΔT) of each glass composition.*

Thermal parameter	S53P4	B12.5	B25	B50
T_g (± 3 °C)	563	532	525	513
T_x (± 3 °C)	710	661	656	679
T_p (± 3 °C)	757/785	757	706	720
$\Delta T = T_x - T_g$ (± 6 °C)	147	129	131	166

The thermal parameters of each borosilicate glass sample were lower than the corresponding values of S53P4, as expected. When comparing the T_g, T_x and T_p values of the borosilicate glasses to each other, it is noticeable that T_g decreases as the B_2O_3 content increases, as it should but T_x and T_p of B50 are higher than the corresponding values of B25. When comparing the thermal processing windows, ΔT increases with the increasing B_2O_3 content, but ΔT for B12.5 and B25 glasses is lower that

of S53P4. When looking at the intensities of the crystallization peaks it can be noticed that the intensity of B12.5 is much higher that of S53P4, but the intensity of B25 is much lower than that of S53P4. For B50 the intensity of the crystallization peak is between S53P4 and B25. S53P4 has two crystallization peaks as expected, but none of the borosilicate glasses show two crystallization peaks although it has been studied that borosilicate glasses likely form two crystal phases [10].

When comparing the results with previous studies [10, 73], the results are mainly in line with the previous results. The main difference is that in the previous studies ΔT values of borosilicate glasses were always larger than that of S53P4. The differences between the results can partially be explained by particle size difference. Smaller particles have a smaller ΔT due to the increase of nucleation sites and the difference in ΔT between S53P4 and borosilicate glasses is also smaller for smaller glass particles, as indicated in study [45].

As B50 has the largest ΔT, it has the most potential to be sintered without it crystallizing and, as was mentioned in Section 2.7, B50, with 125–250 µm particle size, can be sintered without crystal formation. B50 with < 38 µm and 250–500 µm-sized particles can also be sintered without crystal formation, as shown in studies [10, 73]. In addition to B50, B12.5 and B25 can also be sintered without them crystallizing, as shown in studies [10, 12, 73]. So, even though B12.5 and B25, with 125–250 µm particle size, have a smaller ΔT than S53P4, they can most likely be sintered without crystal formation.

4.2 In Vitro Dissolution and Bioactivity

Dissolution tests were carried out by immersing the glass particles in SBF or TRIS for 6–168 h at 37 °C and then the pH of the solution was measured. The tests were carried out to study how B_2O_3 addition effects the dissolution rate and HCA layer formation. The pH of the SBF and TRIS solutions for each glass composition after each time point are presented in Figure 5.

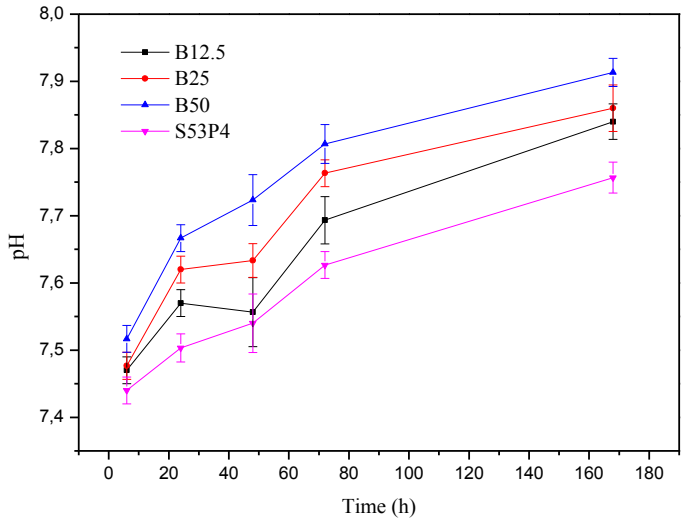

a)

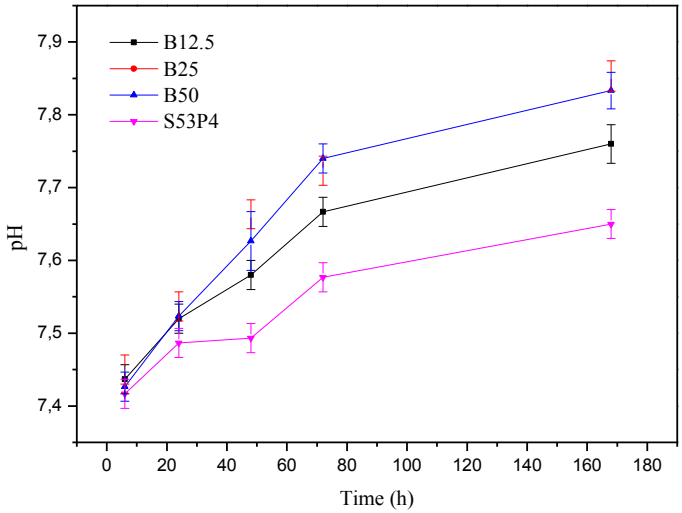

b)

Figure 5. *pH of the a) TRIS and b) SBF solution with glass particles immersed in it after each time point.*

In the dissolution test with TRIS the pH of the solution increased with time and with increasing B_2O_3 content. In TRIS the pH values for B50 are higher than for B25, unlike in SBF indicating that B50 would dissolve quicker than B25. All the measured pH values for TRIS were higher than for SBF indicating that the glasses dissolve quicker in TRIS. In a recent study [74] the effect of chloride ions in TRIS on the dissolution of bioactive glasses was studied. Significantly higher chloride concentration, than from the dissolution of bioactive glasses, can cause hydroxyl in HA to be replaced by chloride, forming a chlorapatite layer [74]. In the study [74], it was found that high chloride concentrations do not cause significant differences in the HA or HCA layer formation.

In the dissolution test with SBF the pH of the solutions increased with time and up to B25, and then interestingly the pH values for B50 are almost the same as for B25 indicating that B50 would dissolve at the same rate as B25. The use of SBF for testing the bioactivity and bone bonding ability of bioactive glasses has been criticized because: (i) The manufacturing procedure is complicated. (ii) The solution is not filtered at any point, which increases the risk of insoluble contaminants. (iii) SBF solution is already supersaturated towards HCA precipitation. [19, 20] Compared to a previous study [75] conducted with 250–500 µm particles, the obtained pH values obtained in this work agree with the previous results.

In both solutions, TRIS and SBF, the dissolution rate is more rapid in the first 72 h and then it slows down, but all in all the dissolution of each glass composition is quite controlled. The borosilicate glasses dissolved quicker than S53P4 in both solutions, which is positive because S53P4 dissolves too slow [10]. B50 dissolves the quickest as the dissolution rate increases with the increasing B_2O_3 content. The formation of the HCA layer is connected to the dissolution, so based on the test results, B50 should form the thickest HCA layer.

The ion release and the dissolution rate of the glass samples was further studied with ICP-OES. Figure 6 presents the percentage of a) B, b) Si, c) Ca, d) Na and e) P ions in TRIS as a function of immersion time. The percentage of ions in SBF and the ionic concentration of each ion in TRIS and SBF as a function of immersion time are presented in Appendix B.

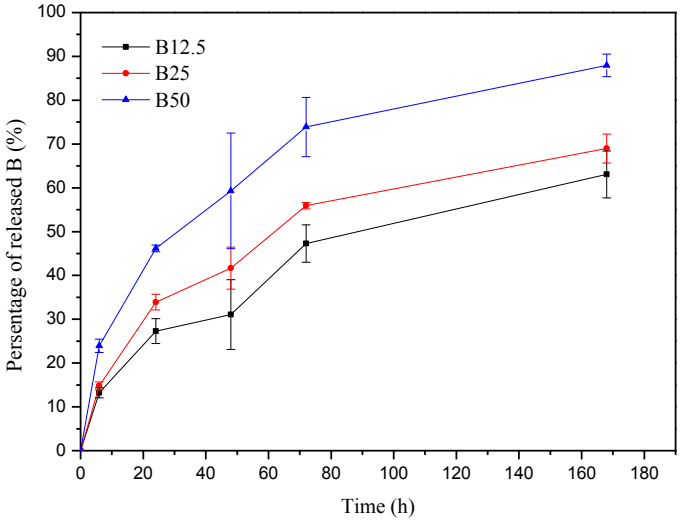
B12.5
B25
B50
Persentage of released B (%)
Time (h)

a)

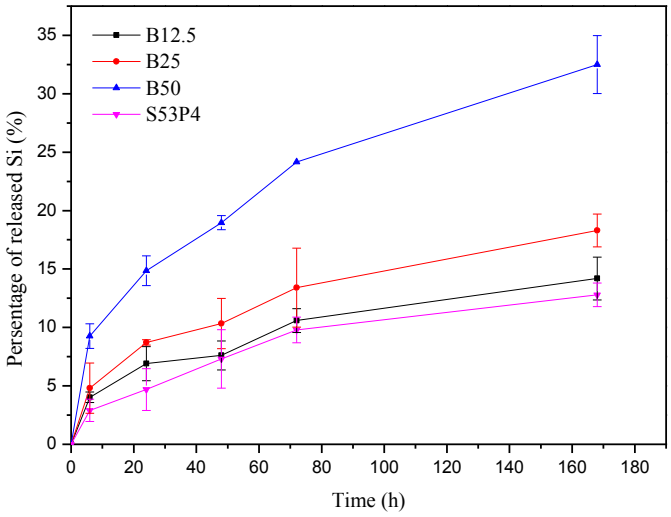
B12.5
B25
B50
S53P4
Persentage of released Si (%)
Time (h)

b)

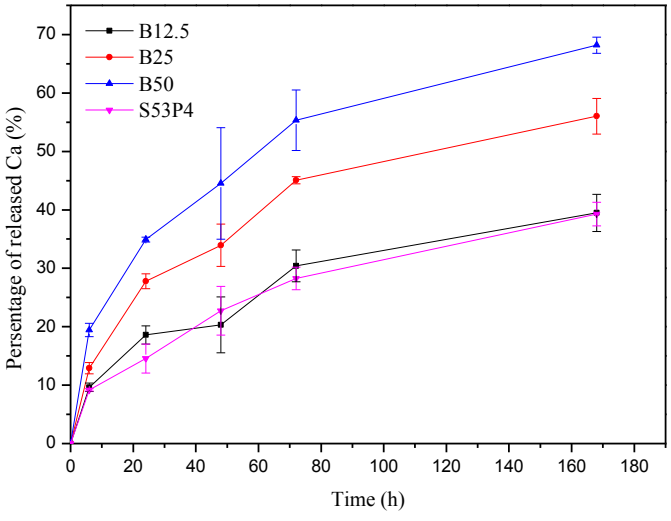
B12.5
B25
B50
S53P4
Persentage of released Ca (%)
Time (h)

c)

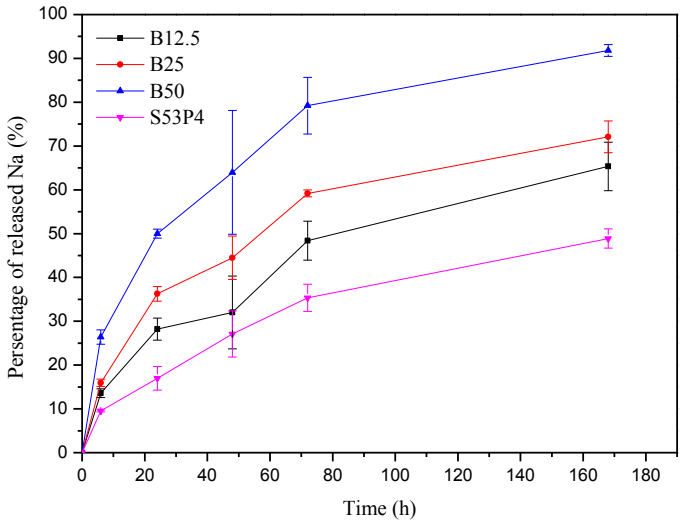

d)

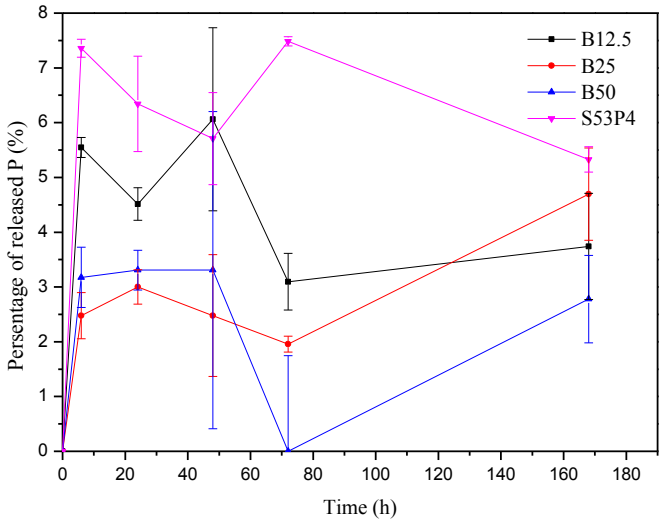

e)

Figure 6. *Percentage of a) B, b) Si, c) Ca, d) Na and e) P ions in TRIS as a function of immersion time.*

Figures 6 a) and b) present the changes is B and Si ions in TRIS, which act as the network formers in the glass structure. The more B_2O_3 there is in the glass, the more it is released into the TRIS solution. It can also be detected that B-O-B bonds are less resistance to hydrolysis than Si-O-Si bonds because only 13–32 % percent of the Si ions in the glass are released in 168 h compared to the 63–88 % of the B ions being released in the same time. The increasing B_2O_3 content also slightly increases the dissolution rate of the silica network because as the B_2O_3 content increases water can more easily get into the glass structure increasing the interaction surface area between water and silicate network. Also, when there is less silica in the glass, the surface to volume ratio of the sub-network increases, which can increase its dissolution rate. [53] Interestingly, when substituting 12.5 % of the SiO_2 with B_2O_3, it causes only a slight 1.4 percentage point (pp) increase in the release of Si ions compared to S53P4 and even when 25 % of the SiO_2 is substituted with B_2O_3 there is also only 4.1 pp difference in the release of B and Si between B25 and B12.5. However, when 50 % of the SiO_2 is substituted with B_2O_3, there is greater 14.2 pp difference in the release of B and Si compared to B25.

Changes in the Ca and Na ion content in TRIS are presented in Figures 6 c) and d). The release of Na ions increases with increasing B_2O_3 content due to the fact that Na in the borate sub-network is released quicker because B in released quicker than Si. Also, Na in the silicate sub-network is released quicker when the B_2O_3 content increases due to more Si being soluble as seen in Figure 6 b). As for Ca ions, the same percentage of Ca ions is released from S53P4 and B12.5, but then for B25 the percentage of released Ca ions increases by 18 % (compared to S53P4 or B12.5). The increase between B25 and B50, in turn, is 19 %. A more thorough structural analysis would be required to evidence the affinity of Ca to enter the silicate or borate sub-network. According to the ICP-OES release curves the release rate of B, Ca, Na and Si ions is more rapid in the first 72 h and then it slows down, as expected. The ion release of P is presented in Figure 6 e). All the release curves differ considerably from each other. With all the other glasses, except for B25, the percentage of released P decreases. Over all, because the percentage of released ions is different for each ion, the dissolution process of the glasses is non-congruent. Pure silica glasses dissolve congruently, which causes excessively long degradation times as S53P4 glass has been found in body even after 14 years of implantation. [10] Borate glasses, in turn, dissolve congruently. Based on the dissolution test and ICP-OES results even though borosilicate glasses dissolve non-congruently their dissolution is quite controlled and quicker than that of S53P4.

Figure 7 presents the ionic concentration of a) B, b) Si, c) Ca, d) Na and e) P ions in SBF as a function of immersion time.

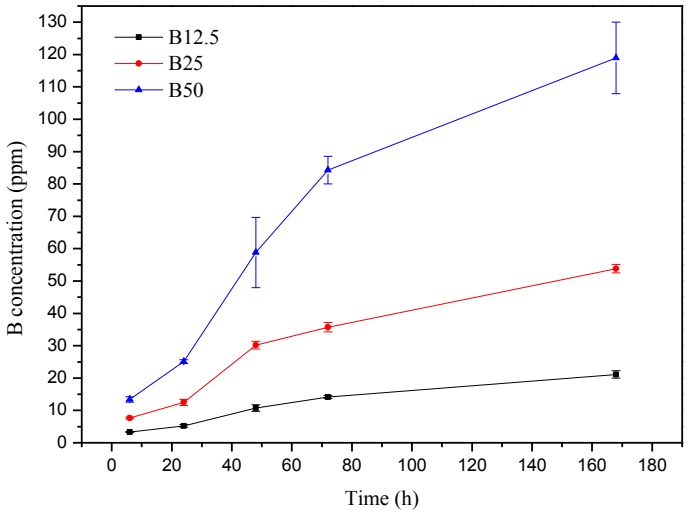

a)

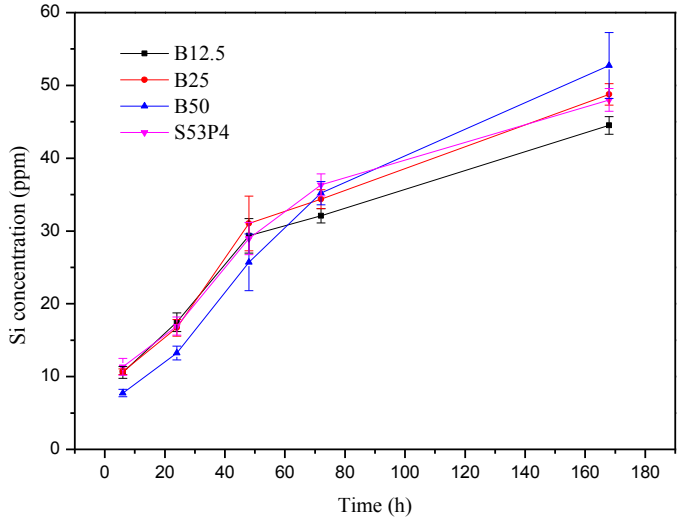
B12.5
B25
B50
S53P4
Si concentration (ppm)
Time (h)

b)

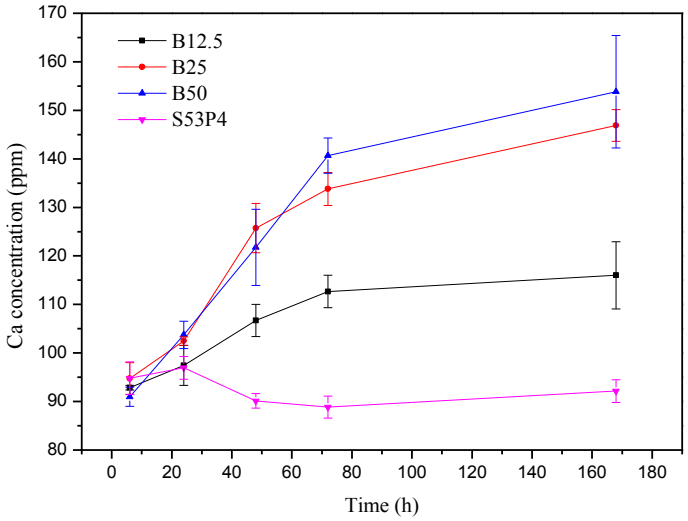
B12.5
B25
B50
S53P4
Ca concentration (ppm)
Time (h)

c)

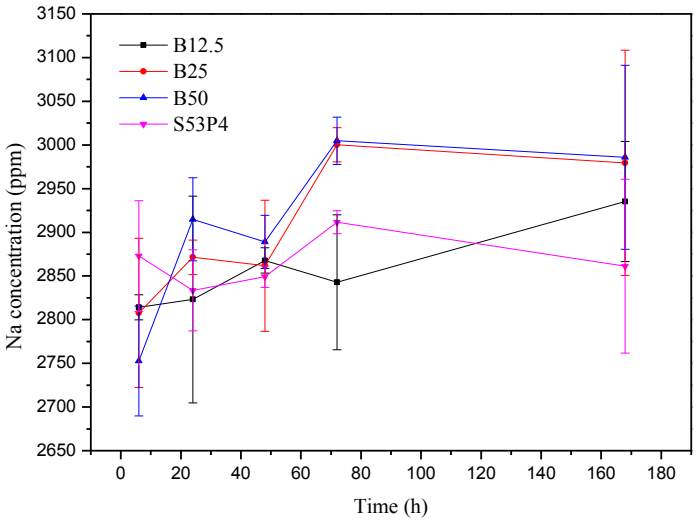
B12.5
B25
B50
S53P4
Na concentration (ppm)
Time (h)

d)

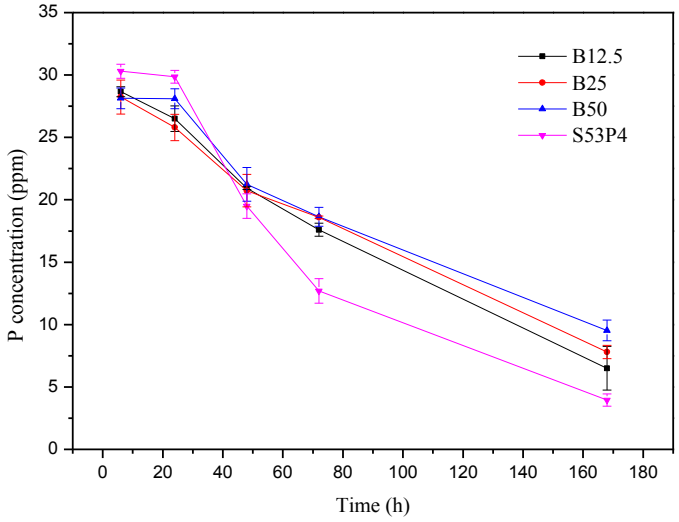

e)

Figure 7. *Ionic concentration (ppm) of a) B, b) Si, c) Ca, d) Na and e) P ions in SBF as a function of immersion time.*

Figures 7 a) and b) present the changes is B and Si ions in SBF. The changes in B and Si ion concentrations in SBF with increasing time are very similar to the ones obtained with TRIS. The concentration B and Si ions is almost the same in SBF and TRIS. Based on the release curves of B and Si in SBF, B50 dissolves quicker than B25 despite its pH did not rise more that of B25.

Changes in the Ca and Na ion in SBF are presented in Figures 7 c) and d). The release curves of Ca for B12.5, B25 and B50 in SBF are slightly different than the corresponding curves for TRIS. The biggest difference is that for S53P4 the concentration of Ca ions decreased during the first 72 h and then it stayed almost the same. Also, less Ca ions were released in TRIS than in SBF. The concentration of Na ions in the SBF solution increased for all the borosilicate glasses and decreased for S53P4. In SBF, the release on Na ions also increased with increasing B_2O_3 content but the differences between the glasses are not as big as in TRIS. The ion release of P in presented in Figure 7 e). The concentration of P ions in the SBF solution decreased for every glass, but the intake rate of the P ions decreased with increasing B_2O_3 content. The release curves of P ions in SBF differ from the ones in TRIS because SBF contains PO_4^{3-} ions, which are used in the formation of the $CaO\text{-}P_2O_5$-rich layer.

When comparing the ionic concentration curves, presented in Figure 7, to the ones obtained in a previous study [75], the ionic concentration curves of B and Ca are very similar in both studies but there are slight differences in the Si and P ion curves. In the study [75], the Si concentration of B25 and B50 started to decrease after 72 h and the P concentration started to increase, which did not happen in this study.

The obtained ICP-OES results support the information obtained from the dissolution tests. The ion release curves show that the dissolution rate increases with increasing, B_2O_3 content, as the percentage of released the B and/or Si ions is highest for B50 and the lowest for S53P4.

The FTIR spectrum of each glass sample was measured after each time point to observe the possible HCA layer formation and how the dissolution affects the surface structure of the glasses. Figure 8

presents the FTIR spectrum of each glass composition before the dissolution tests, and Figure 9 presents the spectrum of S53P4 and B50 after each time point immersed in TRIS or SBF. FTIR spectra of all the glass samples after each time point immersed in TRIS and SBF are presented in Appendix C.

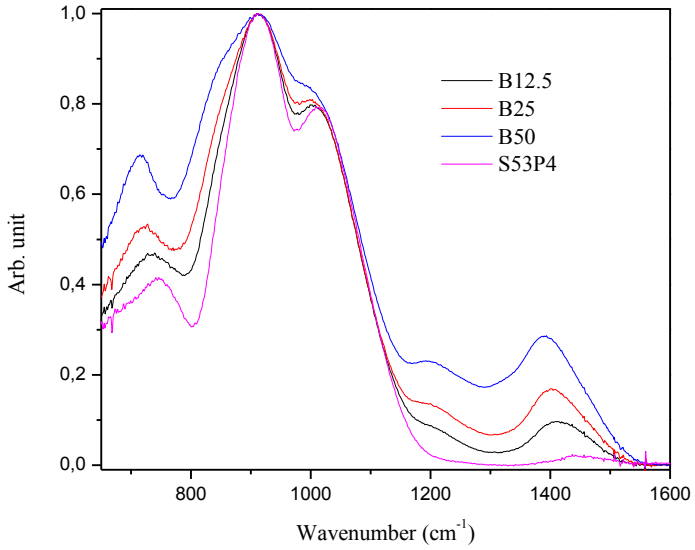

Figure 8. *FTIR spectrum of each glass composition before the dissolution tests.*

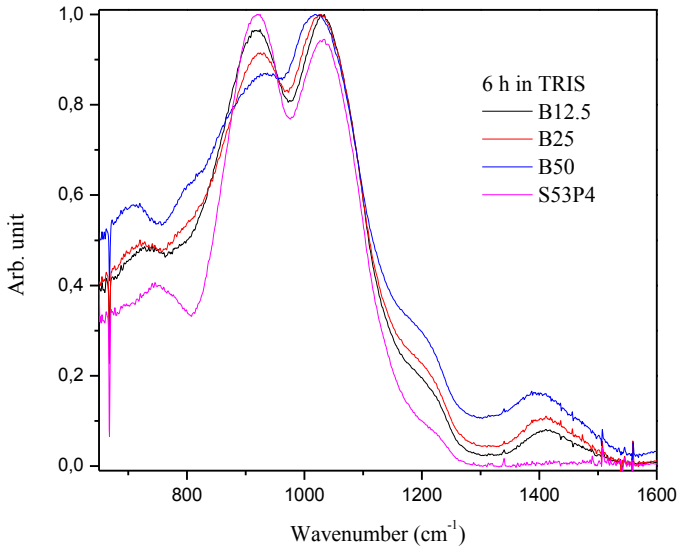

a)

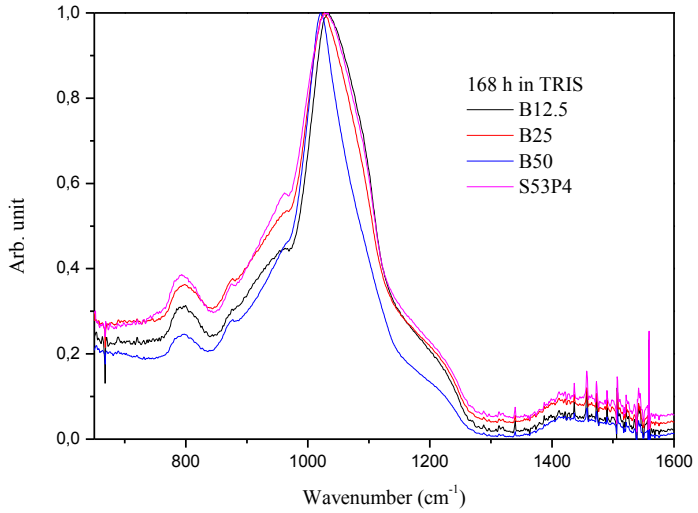
168 h in TRIS
B12.5
B25
B50
S53P4
Arb. unit
Wavenumber (cm-1)
1,0
0,8
0,6
0,4
0,2
0,0
800
1000
1200
1400
1600

b)

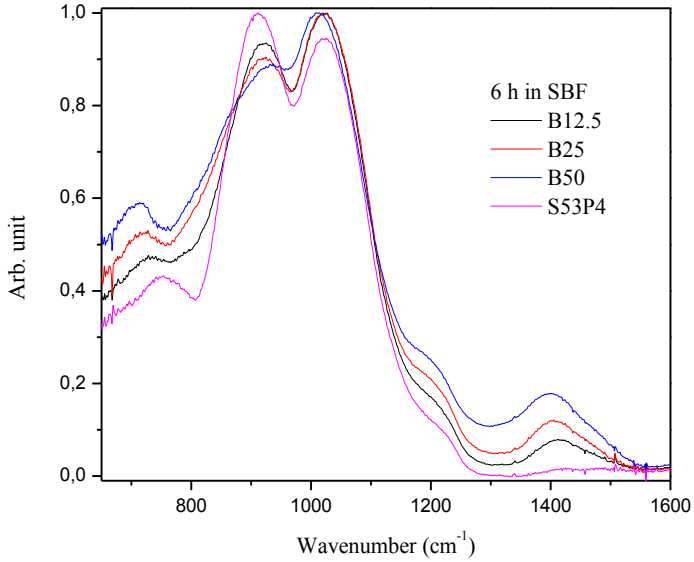
6 h in SBF
B12.5
B25
B50
S53P4
Arb. unit
Wavenumber (cm-1)
1,0
0,8
0,6
0,4
0,2
0,0
800
1000
1200
1400
1600

c)

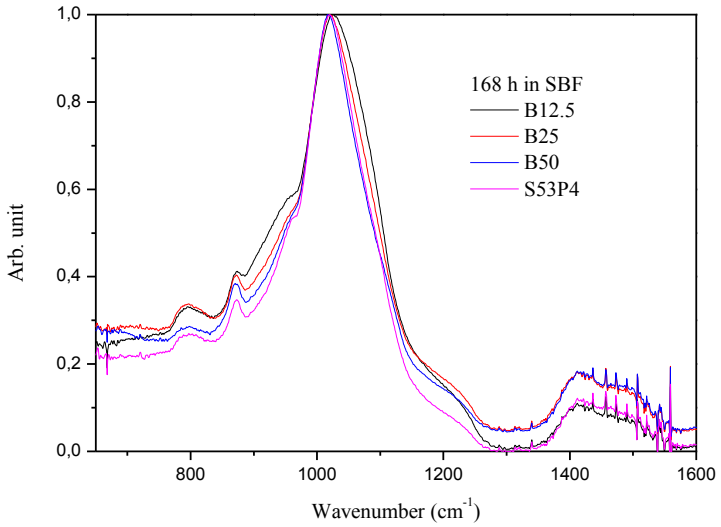

d)

Figure 9. *FTIR spectrum of S53P4 and B50 after each time point immersed in TRIS or SBF.*

For S53P4 a band at 745–800 cm^{-1} is caused by bending vibration of Si-O and symmetric stretching of Si-O-Si bonds in the [SiO_4] tetrahedral. With increasing immersion time, the band shits to a higher wavenumber. A band at 875 cm^{-1}, which appears after 48 h in SBF and after 72 h in TRIS, is caused by CO_3^{2-} in the glass structure, which in bioactive glass is typically assigned to a carbonated reactive layer. A peak at ~930 cm^{-1} is attributed to $Si\text{-}O^-$ stretching of the non-bridging oxygen atoms and it shifts to higher wavenumber and its intensity decreases with increasing immersion time due to the dissolution of the glass network. [10, 20, 76–78] C-O vibrations of the CO_3^{2-} group and P-O-P bonds cause a shoulder at ~ 960 cm-1, which intensity increases with increasing time [77]. A peak at ~1020 cm^{-1} is caused by asymmetric stretching of Si-O-Si bonds and stretching of P-O bonds. The peak at ~1020 cm^{-1} shifts to a higher wavenumber after 6 h and its intensity increases but after 6 h the intensity and the wavenumber stay approximately the same. [10, 20, 76, 77] A band at 1150–1250 cm^{-1} is caused by P=O stretching and the intensity of the band increases with increasing immersion time [78]. Lastly, the band at 1400–1550 cm^{-1} is also caused by CO_3^{2-} in the glass [10, 20, 76, 77]. Overall, the FTIR spectra shows the dissolution of the soluble silica and the precipitation of carbonated calcium phosphate, which can be assigned to HCA in bioactive glasses.

Borosilicate glasses have all the same peaks and bands as S53P4, in addition, to the ones caused by B_2O_3 in the glass network. When B_2O_3 is added, the peaks at ~930 cm^{-1} and ~1020 cm^{-1}, which are caused by vibrations of silica in the glass network, broaden due to vibrations caused by B-O-M (where M stands for a network modifier atom), B-O-Si and B-O-B bonds. [10] With increasing B_2O_3 content: (i) The band at ~745 cm^{-1}, which is caused by vibrations of Si-O and Si-O-Si bonds decreases and shifts to a lower wavenumber forming a new band at 715 cm^{-1} (for B50), which grew in intensity as the B_2O_3 content increased. The new band is caused by bending of the B-O-B bonds and it shifts to a higher wavenumber and its intensity decreases with increasing immersion time. (ii) The intensity of a peak at 875 cm^{-1}, which is caused by vibrations of CO_3^{2-} in HCA, [BO_4] and P-O, increases. The intensity of the peak increases also in time. (iii) A band caused by vibrations of [BO_2O^-] at 1160–1270 cm^{-1} appears and increases in intensity. (iv) A shoulder appears at 1330 cm^{-1}, which is caused by stretching of [BO_3] triangles. (v) The stretching of [BO_3] triangles cause a band at 1300–1550 cm^{-1}, which partially overlaps with the band caused by CO_3^{2-} in HCA at 1400–1550 cm^{-1}. As the B_2O_3

content increases the peak of the band shifts to a lower wavenumber (to 1390 cm^{-1}). With increasing immersion time peak of the band shifts slightly to a higher wavenumber with some of the glass samples. [10, 79] In both solutions, the initial dissolution of the glass backbone is faster with increasing B_2O_3 content.

As seen from Figure 9 b) and d), an HCA layer formed on the surface of each glass composition in TRIS and SBF, but the precipitated HCA layer was thinner in TRIS than in SBF. Based on the dissolution tests and ICE-OES results it seems that the thickness of the formed HCA layer increases with increasing B_2O_3 content. The formed HCA layer of B12.5 is slightly thinner that of S53P4 based on the FTIR results, but the used measuring technique (ATR) can influence the obtained spectra. In ATR, because the glass particles are pressed against the crystal the outermost layer, which is the HCA layer, can be damaged revealing the layer underneath it with a different composition, which changes the obtained spectrum. B50 has the thickest and most crystallized reactive layer on its surface, which can be seen from Figures 9 b) and d). The peak at ~1020 cm^{-1}, which is caused by P-O and Si-O-Si bonds, is the narrowest, and the peak at ~875 cm^{-1}, which is caused by P-O, CO_3^{2-} and $[BO_4]$, has the highest intensity. B50 has the least amount of carbonate present in the formed reactive layer, which can be seen from Figure 9 d). The band at 1400–1500 cm^{-1}, which is caused by CO_3^{2-}, has the lowest intensity. The reason for this anomaly is still unknown. As the difference in the carbon content between the glasses is so small, it most likely does not cause any noticeable differences in interaction between the reactive surface layer and the surrounding tissues and cells.

5. CONCLUSIONS

In this Bachelor of Science thesis, three different borosilicate glass composition based on commercial the S53P4 glass were produced along with S53P4. The glasses' thermal properties, in vitro dissolution and bioactivity were studied to determine which composition would be the most suitable to be used as a tissue engineering scaffold material.

DTA was used to determine the glasses thermal properties. The obtained result for B50 agree with previous studies that out of these four glasses B50 has the widest thermal processing window. In several previous studies conducted with different particle sizes, B50 has successfully been sintered without it crystallizing. The DTA results for B12.5 and B25 did not agree with previous studies, as their thermal processing window was narrower than that of S53P4. In vitro dissolution and bioactivity were studied with dissolution tests in SBF and TRIS, ICP-OES and FTIR. The dissolution test pH-curves showed that borosilicate glasses dissolve quicker than S53P4 and that the dissolution rate increases with increasing B_2O_3 content. In addition, based on the pH curves the dissolution of borosilicate glasses was quite controlled. The ICP-OES and FTIR results supported the information from the pH-curves, and the formation of an HCA layer could clearly be seen from the FTIR spectra. All the obtained results from the dissolution tests mostly agreed with previous results indicating that borosilicate glasses with desired properties can be quite easily reproduced.

Based on all the results, the most promising glass to be used in tissue engineering seems to be B50 because it has the widest ΔT, it dissolves the quickest and it formed the thickest and most crystallized HCA layer on its surface after 168 h.

Overall, borosilicate glasses seem very promising materials for tissue engineering and several studies concerning e.g. scaffold production, addition of magnesium or strontium into the glass network, the use of luminescence particle to enable optical imaging, and how borosilicate glasses and their dissolution products effect human adipose stem cells have already been conducted [10, 12, 75, 80]. However, further cell compatibility studies with glass particles and scaffolds need to be done to fully understand how borosilicate glasses affect cells and to optimize the glass composition.

REFERENCES

[1] F.J. O'Brien, Biomaterials & scaffolds for tissue engineering, Materials Today, Vol. 14, Iss. 3, 2011, pp. 88–95.

[2] M. Puska, A.J. Aho, P.K. Vallittu, Biomateriaalit luuston korjauksessa, Duodecim, Vol. 129, Iss. 5, 2013, pp. 489–496.

[3] P. Törmälä, M. Kellomäki, N. Ashammakhi, R. Suuronen, Kullasta kudosteknologiaan-kohti optimaalista korjausta, Duodecim, Vol. 120, Iss. 16, 2004, pp. 1975–1976.

[4] L.L. Hench, J. Wilson, An Introduction to Bioceramics, World Scientific Publishing Company, 2nd ed., Singapore, 1993, pp. 49–56.

[5] L.L. Hench, The story of Bioglass, Journal of Materials Science: Materials in Medicine, Vol. 17, Iss. 11, 2006, pp. 967–978.

[6] T. Albrektsson, C. Johansson, Osteoinduction, osteoconduction and osseointegration, European Spine Journal, Vol. 10, Iss. S2, 2001, pS101.

[7] J.R. Jones, Review of bioactive glass: From Hench to hybrids, Acta Biomaterialia, Vol. 9, Iss. 1, 2013, pp. 4457–4486.

[8] M.N. Rahaman, D.E. Day, B. Sonny Bal, Q. Fu, S.B. Jung, L.F. Bonewald, A.P. Tomsia, Bioactive glass in tissue engineering, Acta Biomaterialia, Vol. 7, Iss. 6, 2011, pp. 2355–2373.

[9] H. Arstila, E. Vedel, M. Hupa, L. Hupa, Factors affecting crystallization of bioactive glasses, Journal of the European Ceramic Society, Vol. 27, Iss. 2, 2007, pp. 1543–1546.

[10] M. Fabert, N. Ojha, E. Erasmus, M. Hannula, M. Hokka, J. Hyttinen, J. Rocherullé, I. Sigalas, J. Massera, Crystallization and sintering of borosilicate bioactive glasses for application in tissue engineering, JOURNAL OF MATERIALS CHEMISTRY B, Vol. 5, Iss. 23, 2017, pp. 4514–4525.

[11] D.S. Brauer, Bioactive Glasses—Structure and Properties, Angewandte Chemie International Edition, Vol. 54, Iss. 14, 2015, pp. 4160–4181.

[12] J. Pohjola, Borosilicate Scaffold Processing for Bone Tissue Engineering, 2017, Master of Science Thesis, Tampere University of Technology. Available: http://urn.fi/URN:NBN:fi:tty-201710232046.

[13] Amorphous, A Dictionary of Chemistry, 7th ed., Oxford University Press, 2016, webpage. Available (accessed 21.6.2018): http://www.oxfordreference.com.lib-proxy.tut.fi/view/10.1093/acref/9780198722823.001.0001/acref-9780198722823-e-224

[14] Glass, A Dictionary of Chemistry, 7th ed., Oxford University Press, 2016, webpage. Available (accessed 21.6.2018): http://www.oxfordreference.com.lib-proxy.tut.fi/view/10.1093/acref/9780198722823.001.0001/acref-9780198722823-e-1884

[15] M.F. Ashby, H. Shercliff, D. Cebon, I., Materials: engineering, science, processing and design, 2nd; 1st ed., Elsevier/Butterworth-Heinemann, Oxford, 2009, pp. 16–17.

[16] Bioactive Glasses: Fundamentals, Technology and Applications, ProtoView, Ringgold Inc, Beaverton, 2017, 66 p.

[17] Bioactive Glass: A Material for the Future, World Journal of Dentistry, 2012, pp. 199–201.

[18] B.D. Ratner, A.S. Hoffman, F.J. Schoen, J.E. Lemons, Biomaterials Science: An Introduction to Materials in Medicine, 3rd ed., Academic Press, US, 2012, 133 p.

[19] M. Bohner Jacques, Can bioactivity be tested in vitro with SBF solution? Biomaterials, Vol. 30, Iss. 12, 2009, pp. 2175-2179.

[20] A.L.B. Maçon, T.B. Kim, E.M. Valliant, K. Goetschius, R.K. Brow, D.E. Day, A. Hoppe, A.R. Boccaccini, I.Y. Kim, C. Ohtsuki, T. Kokubo, A. Osaka, M. Vallet-Regí, D. Arcos, L. Fraile, A.J. Salinas, A.V. Teixeira, Y. Vueva, R.M. Almeida, M. Miola, C. Vitale-Brovarone, E. Verné, W. Höland, J.R. Jones, A unified in vitro evaluation for apatite-forming ability of bioactive glasses and their variants, Journal of Materials Science: Materials in Medicine, Vol. 26, Iss. 2, 2015, pp. 1-10.

[21] O. Leppäranta, M. Vaahtio, T. Peltola, D. Zhang, L. Hupa, M. Hupa, H. Ylänen, J.I. Salonen, K. Viljanen, E. Eerola, Antibacterial effect of bioactive glasses on clinically important anaerobic bacteria in vitro, Journal of Materials Science: Materials in Medicine, Vol. 19, Iss. 2, 2008, pp.547–551.

[22] E. Munukka, O. Leppäranta, M. Korkeamäki, M. Vaahtio, T. Peltola, D. Zhang, L. Hupa, H. Ylänen, J.I. Salonen, M.K. Viljanen, E. Eerola, Bactericidal effects of bioactive glasses on clinically important aerobic bacteria, Journal of Materials Science: Materials in Medicine, Vol. 19, Iss. 1, 2008, pp. 27–32. [21] Osteogenesis, A Dictionary of Biomedicine, 1st ed., Oxford University Press, 2010.

[23] osteogenesis, in: A Dictionary of Biomedicine, 1st ed., Oxford University Press, 2010, webpage. Available (accessed 13.8.2018): http://www.oxfordreference.com.lib-proxy.tut.fi/view/10.1093/acref/9780199549351.001.0001/acref-9780199549351-e-6876

[24] R.B. Heimann, H.D. Lehmann, Bioceramic Coatings for Medical Implants: Trends and echniques, Wiley-VCH, DE, 2015, 57 p.

[25] 510(k) SUMMARY Inion BioRestore™, U.S. Food and Drug Administration, 2009. Available: https://www.accessdata.fda.gov/scripts/cdrh/cfdocs/cfPMN/pmn.cfm?ID=K090177.

[26] W. Liang, M.N. Rahaman, D.E. Day, N.W. Marion, G.C. Riley, J.J. Mao, Bioactive borate-glass scaffold for bone tissue engineering, Journal of Non-Crystalline Solids, Vol. 354, Iss. 15-16, 2008, pp. 1690–1696.

[27] Autograft, Concise Medical Dictionary, 9th ed., Oxford University Press, 2015, webpage. Available (accessed 30.6.2018): http://www.oxfordreference.com.lib-proxy.tut.fi/view/10.1093/acref/9780199687817.001.0001/acref-9780199687817-e-851

[28] Allograft, Concise Medical Dictionary, 9th ed., Oxford University Press, 2015, webpage. Available (accessed 30.6.2018): http://www.oxfordreference.com.lib-proxy.tut.fi/view/10.1093/acref/9780199687817.001.0001/acref-9780199687817-e-299

[29] Xenograft, Concise Medical Dictionary, 9th ed., Oxford University Press, 2015, webpage. Available (accessed 30.6.2018): http://www.oxfordreference.com.lib-proxy.tut.fi/view/10.1093/acref/9780199687817.001.0001/acref-9780199687817-e-10944

[30] J.M. Anderson, A. Rodriguez, D.T. Chang, Foreign body reaction to biomaterials, Seminars in immunology, Vol. 20, Iss. 2, 2008, pp. 86–100.

[31] R. Klopfleisch, F. Jung, The pathology of the foreign body reaction against biomaterials, Journal of Biomedical Materials Research Part A, Vol. 105, Iss. 3, 2017, pp. 927–940.

[32] T. Jiang, R. James, S.G. Kumbar, C.T. Laurencin, Chitosan as a Biomaterial: Structure, Properties, and Applications in Tissue Engineering and Drug Delivery, Natural and Synthetic Biomedical Polymers, Elsevier Inc., 2014, pp. 91–107.

[33] L.C. De Jonghe, M.N. Rahaman, Sintering of Ceramics, Handbook of Advanced Ceramics, Vol. 1, Elsevier Inc., 2003, pp. 187–264.

[34] H. Djohari, J.I. Martínez-Herrera, J.J. Derby, Transport mechanisms and densification during sintering: I. Viscous flow versus vacancy diffusion, Chemical Engineering Science, Vol. 64, Iss. 17, 2009, pp. 3799–3809.

[35] T. Lever, P. Haines, J. Rouquerol, E.L. Charsley, P.V. Eckeren, D.J. Burlett, ICTAC nomenclature of thermal analysis (IUPAC Recommendations 2014), Pure and Applied Chemistry. Chimie Pure et Appliquee, Vol. 86, Iss. 4, 2014, 545 p.

[36] Differential Scanning Calorimetry (DSC) Frequently Asked Questions, PerkinElmer Inc. Available (accessed 9.7.2018): http://www.perkinelmer.com/fi/category/differential-scanning-calorimetry-dsc-instruments.

[37] Glass transition, A Dictionary of Physics, 7th ed., Oxford University Press, 2015, webpage. Available (accessed 10.7.2018): http://www.oxfordreference.com.libproxy.tut.fi/view/10.1093/acref/9780198714743.001.0001/acref-9780198714743-e-3412

[38] G. Grest, Glass transition, AccessScience, McGraw-Hill Education, 2014. Available (accessed 10.7.2018): https://www.accessscience.com/content/290850

[39] L.H. Sperling, Introduction to Physical Polymer Science, Wiley, Hoboken, 2005, 349 p.

[40] Glass transition temperature, A Dictionary of Mechanical Engineering, 1st ed., Oxford University Press, 2013, webpage. Available (accessed 10.7.2018): http://www.oxfordreference.com.libproxy.tut.fi/view/10.1093/acref/9780199587438.001.0001/acref-9780199587438-e-2638

[41] Metastable state, A Dictionary of Chemistry, 7th ed., Oxford University Press, 2016, webpage. Available (accessed 10.7.2018): http://www.oxfordreference.com.libproxy.tut.fi/view/10.1093/acref/9780198722823.001.0001/acref-9780198722823-e-2685

[42] P.G. Vekilov, Nucleation, Crystal Growth and Design, Vol. 10, Iss. 12, 2010, pp. 5007–5019.

[43] V. Marghussian, Glass Crystallization, Nano-Glass Ceramics, Elsevier Inc, 2015, pp. 1-62.

[44] J. Massera, S. Fagerlund, L. Hupa, M. Hupa, L. Pinckney, Crystallization Mechanism of the Bioactive Glasses, 45S5 and S53P4, Journal of the American Ceramic Society, Vol. 95, Iss. 2, 2012, pp. 607-613.

[45] E.P. Erasmus, O.T. Johnson, I. Sigalas, J. Massera, Effects of Sintering Temperature on Crystallization and Fabrication of Porous Bioactive Glass Scaffolds for Bone Regeneration, SCIENTIFIC REPORTS, Vol. 7, Iss. 1, 2017, pp. 1–12.

[46] S. Kanehashi, A. Kusakabe, S. Sato, K. Nagai, Analysis of permeability; solubility and diffusivity of carbon dioxide; oxygen; and nitrogen in crystalline and liquid crystalline polymers, Journal of Membrane Science, Vol. 365, Iss. 1, 2010, pp. 40–51.

[47] W. Huang, M. N. Rahaman, D. E. Day, Y. Li, Mechanisms for Converting Bioactive Silicate, Borate, and Borosilicate Glasses to Hydroxyapatite in Dilute Phosphate Solution, Physics and Chemistry of Glasses - European Journal of Glass Science and Technology Part B, Vol. 47, 2006, pp. 647–658.

[48] W. Huang, D.E. Day, K. Kittiratanapiboon, M.N. Rahaman, Kinetics and mechanisms of the conversion of silicate (45S5), borate, and borosilicate glasses to hydroxyapatite in dilute phosphate solutions, Journal of Materials Science: Materials in Medicine, Vol. 17, Iss. 7, 2006, pp. 583–596.

[49] Q. Fu, M.N. Rahaman, H. Fu, X. Liu, Silicate, borosilicate, and borate bioactive glass scaffolds with controllable degradation rate for bone tissue engineering applications. I. Preparation and in vitro degradation, Journal of Biomedical Materials Research Part A, Vol. 95A, Iss. 1, 2010, pp. 164–171.

[50] H. Fu, Q. Fu, N. Zhou, W. Huang, M.N. Rahaman, D. Wang, X. Liu, In vitro evaluation of borate-based bioactive glass scaffolds prepared by a polymer foam replication method, Materials Science & Engineering C, Vol. 29, Iss. 7, 2009, pp. 2275–2281.

[51] Q. Fu, M.N. Rahaman, B.S. Bal, L.F. Bonewald, K. Kuroki, R.F. Brown, Silicate, borosilicate, and borate bioactive glass scaffolds with controllable degradation rate for bone tissue engineering applications. II. In vitro and in vivo biological evaluation, Journal of Biomedical Materials Research Part A, Vol. 95A, Iss. 1, 2010, pp. 172–179.

[52] A. Yao, D. Wang, W. Huang, Q. Fu, M.N. Rahaman, D.E. Day, In Vitro Bioactive Characteristics of Borate- Based Glasses with Controllable Degradation Behavior, Journal of the American Ceramic Society, Vol. 90, Iss. 1, 2007, pp. 303–306.

[53] J. George, Dissolution of borate glasses and precipitation of phosphate compounds, 2015, Doctoral Dissertation, Missouri University of Science and Technology, pp. 4–7, 42–43. Available: http://scholarsmine.mst.edu/doctoral_dissertations/2382.

[54] A. Hoppe, N.S. Güldal, A.R. Boccaccini, A review of the biological response to ionic dissolution products from bioactive glasses and glass-ceramics, Biomaterials, Vol. 32, Iss. 11, 2011, pp. 2757–2774.

[55] L.A. Haro Durand, G.E. Vargas, N.M. Romero, R. Vera-Mesones, J.M. Porto-López, A.R. Boccaccini, M.P. Zago, A. Baldi, A. Gorustovich, Angiogenic effects of ionic dissolution products released from a boron-doped 45S5 bioactive glass, Journal of Materials Chemistry B, Vol. 3, Iss. 6, 2015, pp. 1142–1148.

[56] S. Fagerlund, J. Massera, N. Moritz, L. Hupa, M. Hupa, Phase composition and in vitro bioactivity of porous implants made of bioactive glass S53P4, Acta Biomaterialia, Vol. 8, Iss. 6, 2012, pp. 2331-2339.

[57] O. Peitl Filho, G.P. LaTorre, L.L. Hench, Effect of crystallization on apatite-layer formation of bioactive glass 45S5, Journal of biomedical materials research, Vol. 30, Iss. 4, 1996, pp. 509-514.

[58] G. Kaur, Biomedical, therapeutic and clinical applications of bioactive glasses, Woodhead Publishing, Elsevier Inc, 2018, 223 p.

[59] J. Massera, C. Claireaux, T. Lehtonen, J. Tuominen, M. Hupa, L. Hupa, Control of the thermal properties of slow bioresorbable glasses by boron addition, Journal of Non-Crystalline Solids, Vol. 357, Iss. 21, 2011, pp. 3623–3630.

[60] G. Kaur, Bioactive Glasses: Potential Biomaterials for Future Therapy, Springer, Cham, 2017, 129 p.

[61] Annealing, A Dictionary of Physics, 7th ed., Oxford University Press, 2015, webpage. Available (accessed 25.7.2018): http://www.oxfordreference.com.lib-proxy.tut.fi/view/10.1093/acref/9780198714743.001.0001/acref-9780198714743-e-116

[62] Annealing, A Dictionary of Chemistry, 7th ed., Oxford University Press, 2016, webpage. Available (accessed 25.7.2018): http://www.oxfordreference.com.lib-proxy.tut.fi/view/10.1093/acref/9780198722823.001.0001/acref-9780198722823-e-266

[63] Y. Leng, Materials Characterization: Introduction to Microscopic and Spectroscopic Methods, 1. Aufl.; Second ed. Wiley, DE, 2013, pp. 337–339.

[64] P.J. Haines, M. Reading, F.W. Wilburn, Chapter 5 Differential Thermal Analysis and Differential Scanning Calorimetry, Handbook of Thermal Analysis and Calorimetry, Vol. 1, Elsevier Inc., 1998, pp. 279–361.

[65] T. Kokubo, H. Kushitani, S. Sakka, T. Kitsugi, T. Yamamuro, Solutions able to reproduce in vivo surface-structure changes in bioactive glass-ceramic A-W, Journal of Biomedical Materials Research, Vol. 24, Iss. 6, 1990, pp. 721-734.

[66] J.W. OLESIK, 10.9 - ICP-OES: Inductively Coupled Plasma-Optical Emission Spectroscopy, 1992, pp. 633–644.

[67] M. Huang, G.M. Hieftje, Simultaneous measurement of spatially resolved electron temperatures, electron number densities and gas temperatures by laser light scattering from the ICP, Spectrochimica Acta Part B: Atomic Spectroscopy, Vol. 44, Iss. 8, 1989, pp. 739–749.

[68] ICP-OES Sample Preparation, Thermo Fisher Scientific, web page. Available (accessed 30.08.2018): https://www.thermofisher.com/uk/en/home/industrial/spectroscopy-elemental-isotope-analysis/spectroscopy-elemental-isotope-analysis-learning-center/trace-elemental-analysis-tea-information/icp-oes-information/icp-oes-sample-preparation.html.

[69] P. Gaines, ICP Operation Guide, Inorganic Ventures Inc, 2011.Available: https://www.inorganicventures.com/icp-operations-guide

[70] A. Dutta, Chapter 4 – Fourier Transform Infrared Spectroscopy, Spectroscopic Methods for Nanomaterials Characterization, Elsevier Inc, 2017, pp. 73–93.

[71] A.A. Ismail, F.R. van de Voort, J. Sedman, Chapter 4 – Fourier transform infrared spectroscopy: Principles and applications, Instrumental Methods in Food Analysis, Elsevier Science B.V., 1997, pp. 93–139.

[72] N. Jaggi, D.R. Vij, Chapter 9 – Fourier Transform Infrared Spectroscopy, Handbook of Applied Solid State Spectroscopy, Springer US, Boston, MA, 2006, pp. 411–450.

[73] N. Ojha, Borosilicate glass with enhanced hot forming properties and conversion to hydroxyapatite, 2016, Master of Science Thesis, Tampere University of Technology. Available: http://urn.fi/URN:NBN:fi:tty-201606174270.

[74] G. Kirste, J. Brandt- Slowik, C. Bocker, M. Steinert, R. Geiss, D.S. Brauer, Effect of chloride ions in Tris buffer solution on bioactive glass apatite mineralization, International Journal of Applied Glass Science, Vol. 8, Iss. 4, 2017, pp. 438-449.

[75] M. Ojansivu, A. Mishra, S. Vanhatupa, M. Juntunen, A. Larionova, J. Massera, S. Miettinen, The effect of S53P4-based borosilicate glasses and glass dissolution products on the osteogenic commitment of human adipose stem cells, PloS one, Vol. 13, Iss. 8, 2018.

[76] J. Massera, L. Hupa, Influence of SrO substitution for CaO on the properties of bioactive glass S53P4, Journal of Materials Science: Materials in Medicine, Vol. 25, Iss. 3, 2014, pp. 657-668.

[77] J. Massera, M. Hupa, L. Hupa, Influence of the partial substitution of CaO with MgO on the thermal properties and in vitro reactivity of the bioactive glass S53P4, Journal of Non-Crystalline Solids, Vol. 358, Iss. 18-19, 2012, pp. 2701-2707.

[78] H.A. ElBatal, M.A. Azooz, E.M.A. Khalil, A. Soltan Monem, Y.M. Hamdy, Characterization of some bioglass–ceramics, Materials Chemistry and Physics, Vol. 80, Iss. 3, 2003, pp. 599-609.

[79] S.Y. Marzouk, R. Seoudi, D.A. Said, M.S. Mabrouk, Linear and non-linear optics and FTIR characteristics of borosilicate glasses doped with gadolinium ions, Optical Materials, Vol. 35, Iss. 12, 2013, pp. 2077-2084.

[80] H. Teitinen, Pysyvien luminesenssipartikkleidn vaikutus bioaktiivisen borosilikaattilasin ominaisuuksiin, 2018, Bachelor of Science Thesis, Tampere University of Technology. Available: http://urn.fi/URN:NBN:fi:tty-201805241806

APPENDIX A: PRODUCTION OF SBF

1 liter of SBF solution for the dissolutions test was produced by adding the reagents shown in Table A.1 5 to 700 ml of distilled water. The reagents were added slowly into the water letting each reagent to fully dissolve before adding the next. Approximately 35 ml of 1 M HCl was added into the solution after the $MgCl_2$ and the rest of the HCl was reserved for adjusting the pH to 7.40 ± 0.02 at 37.0 ± 0.2 °C after each reagent was dissolved. After the pH was adjusted, the volume was adjusted to 1 liter.

Table A.1. *Reagents and the amounts needed to produce SBF.*

Order	**Reagent**	**Amount**
1	NaCl	7.996 g
2	$NaHCO_3$	0.350 g
3	KCl	0.224 g
4	$K_2HPO_4 \cdot 6H_2O$	0.228 g
5	$MgCl_2$	0.305 g
6	HCl (1M)	~40 ml
7	$CaCl_2 \cdot 2H_2O$	0.368 g
8	Na_2SO_4	0.071 g
9	$(CH_2OH)_3CNH_2$	6.057 g

APPENDIX B: ICP-OES RESULTS

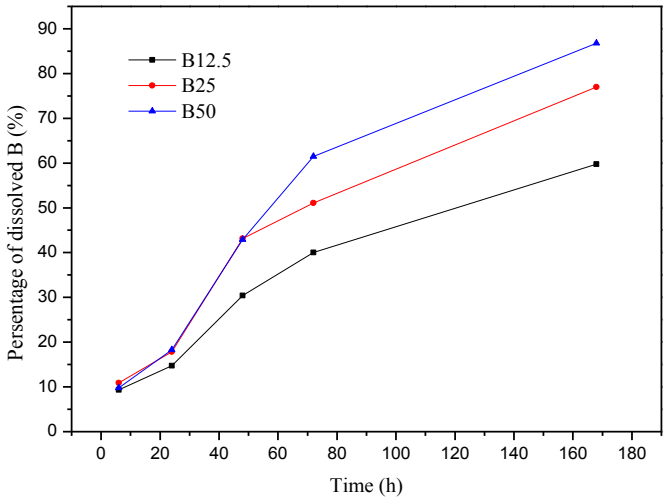

1)

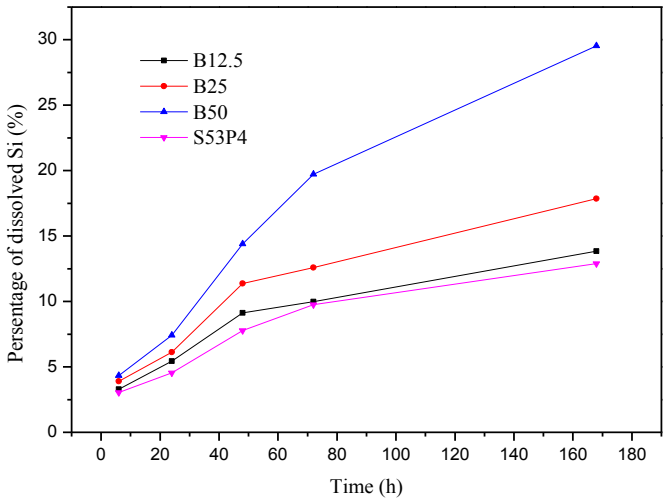

2)

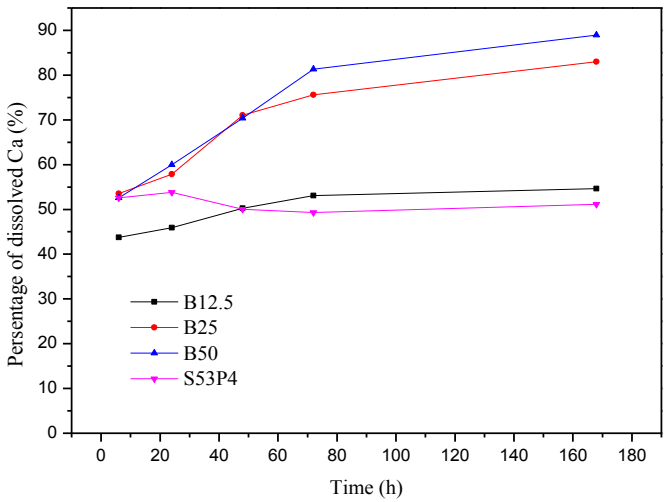

3)

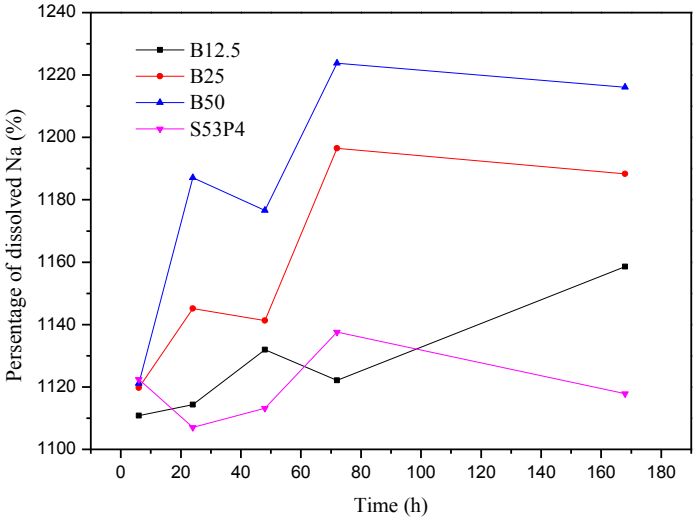

4)

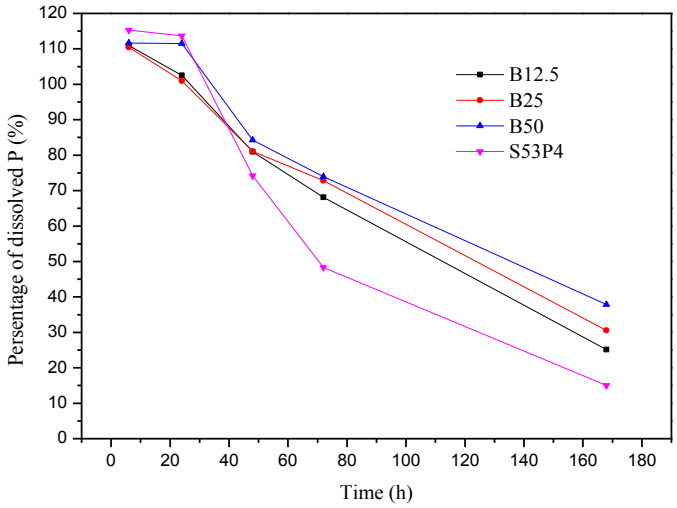

5)

Figure B.1. *Percentage of 1) B, 2) Si, 3) Ca, 4) Na and 5) P ions in SBF as a function of immersion time.*

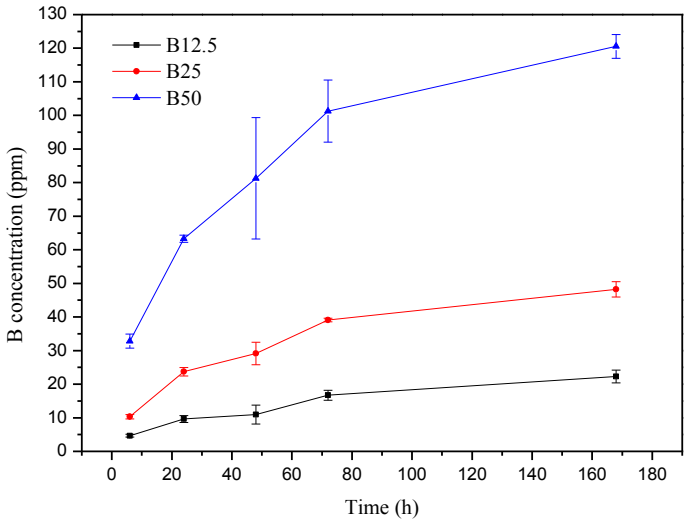
B12.5
B25
B50
B concentration (ppm)
Time (h)

1)

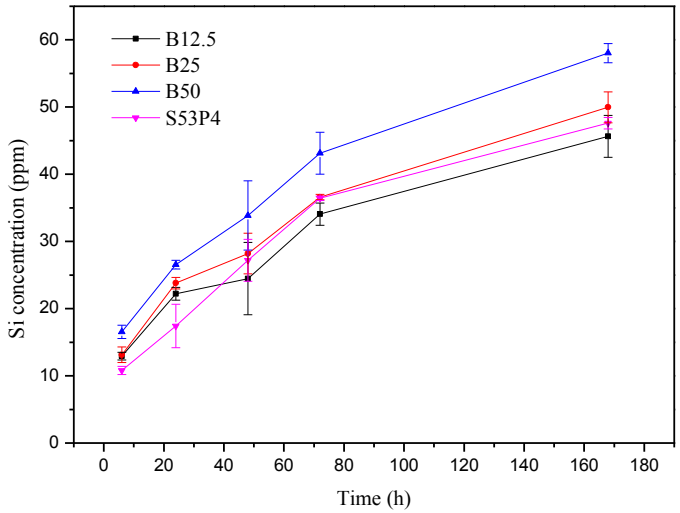
B12.5
B25
B50
S53P4
Si concentration (ppm)
Time (h)

2)

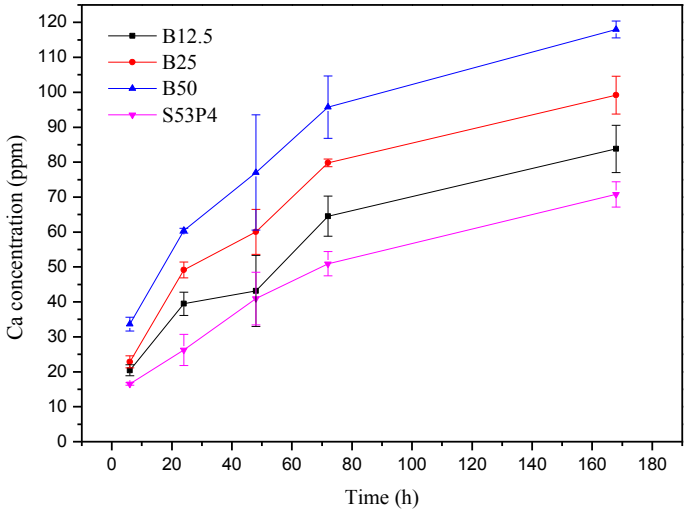
B12.5
B25
B50
S53P4
Ca concentration (ppm)
Time (h)

3)

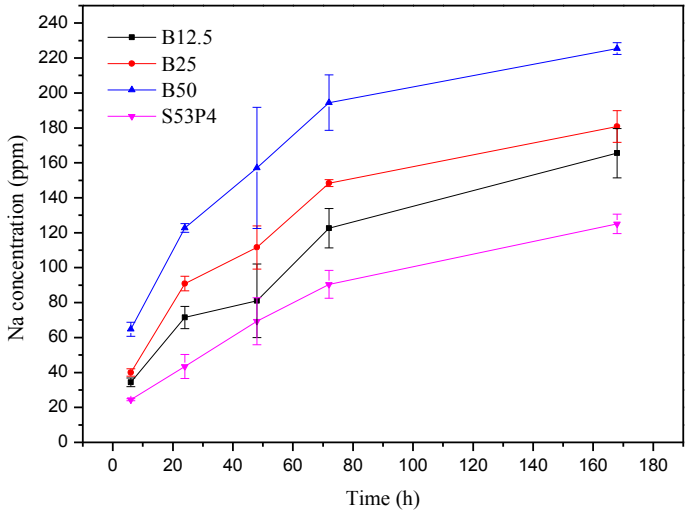

4)

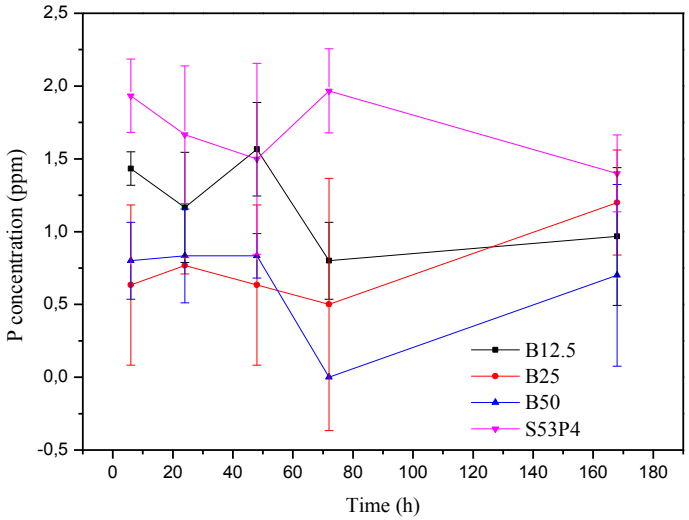

5)

Figure B.2. *Ionic concentration (ppm) of 1) B, 2) Si, 3) Ca, 4) Na and 5) P ions in TRIS as a function of immersion time.*

APPENDIX C: FTIR SPECTRA

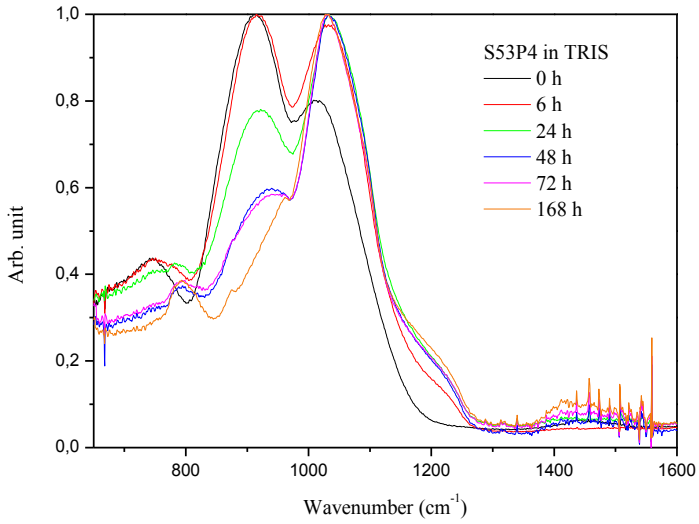

1)

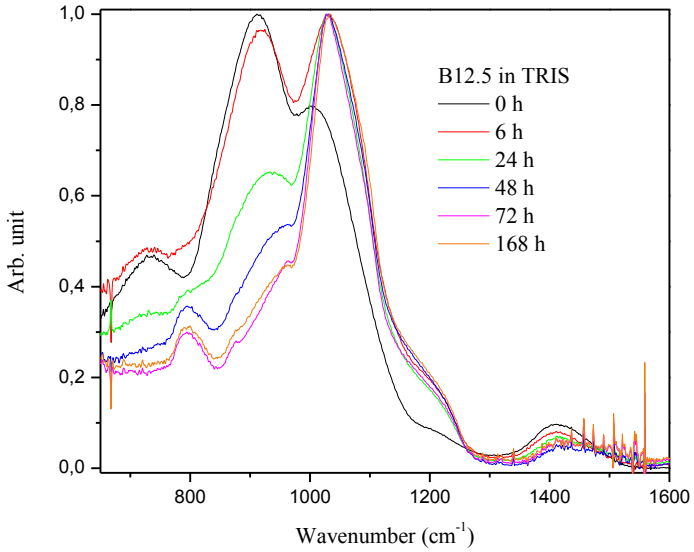

2)

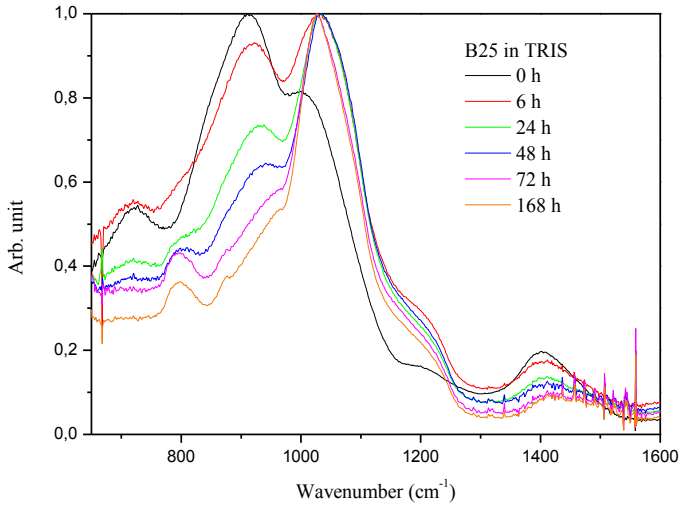

3)

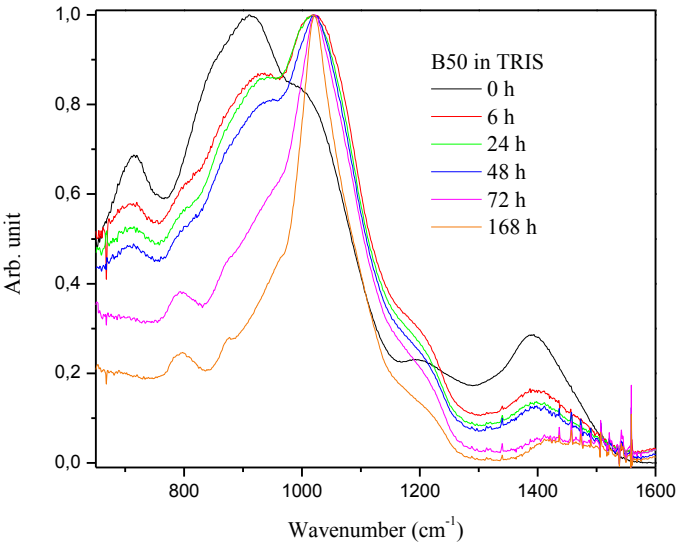

4)

Figure C.1. *FTIR spectrum of 1) S53P4, 2) B12.5, 3) B25 and 4) B50 after each time point immersed in TRIS.*

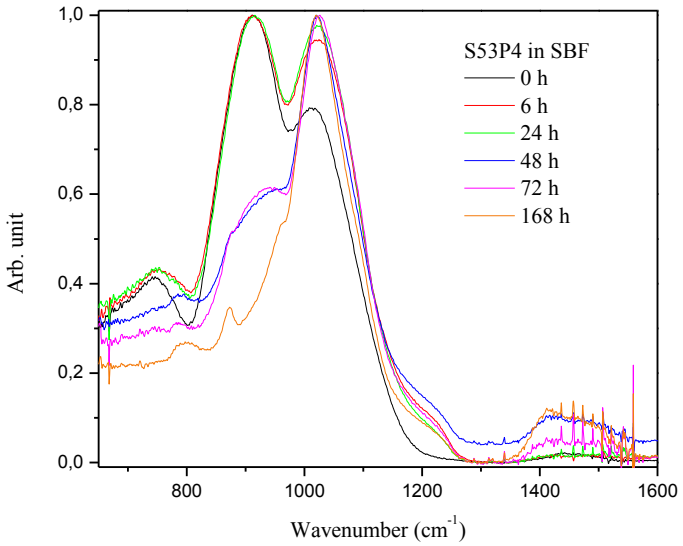
S53P4 in SBF
0 h
6 h
24 h
48 h
72 h
168 h
Arb. unit
Wavenumber (cm-1)
1,0
0,8
0,6
0,4
0,2
0,0
800
1000
1200
1400
1600

1)

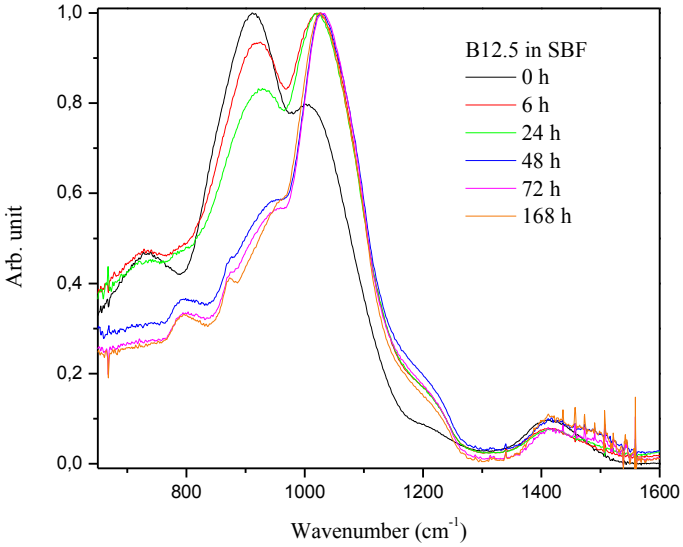
B12.5 in SBF
0 h
6 h
24 h
48 h
72 h
168 h
Arb. unit
Wavenumber (cm-1)
1,0
0,8
0,6
0,4
0,2
0,0
800
1000
1200
1400
1600

2)

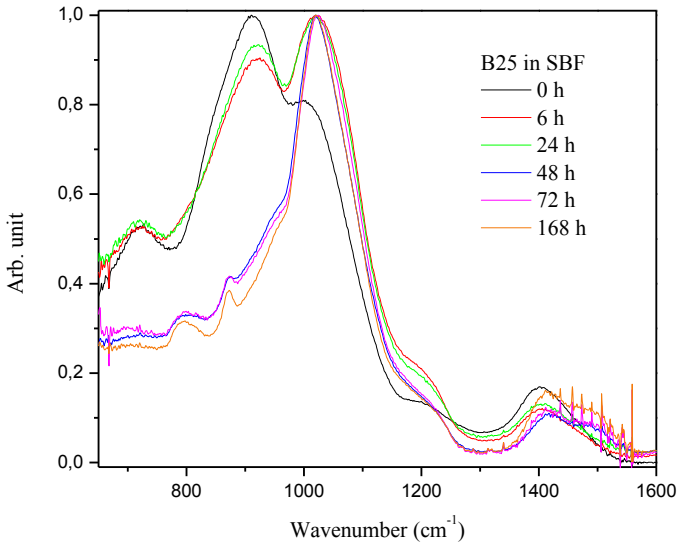

3)

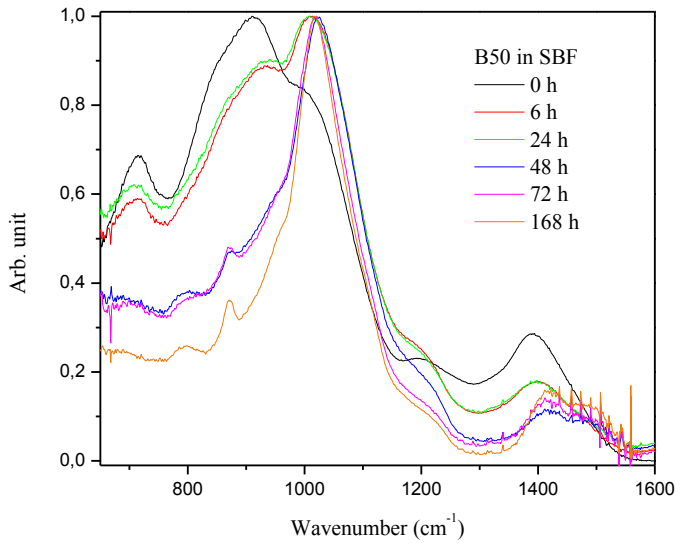

4)

Figure C.2. *FTIR spectrum of 1) S53P4, 2) B12.5, 3) B25 and 4) B50 after each time point immersed in SBF.*